ORIGINAL RESEARCH

Serine/Threonine-Protein Kinase 3 Facilitates Myocardial Repair After Cardiac Injury Possibly Through the Glycogen Synthase Kinase-3β/β-Catenin Pathway

Ya-Fei Li [iD], PhD*; Tian-Wen Wei, PhD*; Yi Fan [iD], PhD*; Tian-Kai Shan, PhD; Jia-Teng Sun, MD; Bing-Rui Chen, PhD; Zi-Mu Wang, PhD; Ling-Feng Gu, MD; Tong-Tong Yang, PhD; Liu Liu, PhD; Chong Du, MD; Yao Ma, MD; Hao Wang, PhD; Rui Sun, PhD; Yong-Yue Wei [iD], PhD; Feng Chen [iD], PhD; Xue-Jiang Guo [iD], PhD; Xiang-Qing Kong, MD, PhD; Lian-Sheng Wang [iD], MD, PhD

BACKGROUND: The neonatal heart maintains its entire regeneration capacity within days after birth. Using quantitative phospho-proteomics technology, we identified that SGK3 (serine/threonine-protein kinase 3) in the neonatal heart is highly expressed and activated after myocardial infarction. This study aimed to uncover the function and related mechanisms of SGK3 on cardiomyocyte proliferation and cardiac repair after apical resection or ischemia/reperfusion injury.

METHODS AND RESULTS: The effect of SGK3 on proliferation and oxygen glucose deprivation/reoxygenation– induced apoptosis in isolated cardiomyocytes was evaluated using cardiomyocyte-specific SGK3 overexpression or knockdown adenovirus5 vector. In vivo, gain- and loss-of-function experiments using cardiomyocyte-specific adeno-associated virus 9 were performed to determine the effect of SGK3 in cardiomyocyte proliferation and cardiac repair after apical resection or ischemia/reperfusion injury. In vitro, overexpression of SGK3 enhanced, whereas knockdown of SGK3 decreased, the cardiomyocyte proliferation ratio. In vivo, inhibiting the expression of SGK3 shortened the time window of cardiac regeneration after apical resection in neonatal mice, and overexpression of SGK3 significantly promoted myocardial repair and cardiac function recovery after ischemia/reperfusion injury in adult mice. Mechanistically, SGK3 promoted cardiomyocyte regeneration and myocardial repair after cardiac injury by inhibiting GSK-3β (glycogen synthase kinase-3β) activity and upregulating β-catenin expression. SGK3 also upregulated the expression of cell cycle promoting genes G1/S-specific cyclin-D1, c-myc (cellular-myelocytomatosis viral oncogene), and cdc20 (cell division cycle 20), but downregulated the expression of cell cycle negative regulators cyclin kinase inhibitor P 21 and cyclin kinase inhibitor P 27.

CONCLUSIONS: Our study reveals a key role of SGK3 on cardiac repair after apical resection or ischemia/reperfusion injury, which may reopen a novel therapeutic option for myocardial infarction.

Key Words: cardiac protection ■ cardiomyocyte proliferation ■ myocardial infarction ■ SGK3

Myocardial infarction (MI), the most serious manifestation of ischemic heart disease, could induce irreversible death of cardiomyocytes in the infarcted area, leading to ventricular remodeling, heart failure, and even death.[1] At present, myocardial ischemia/reperfusion (I/R) injury therapy could improve the blood supply of myocardial tissue after MI, but could not regenerate the necrotic myocardial

CLINICAL PERSPECTIVE

What Is New?

- SGK3 (serine/threonine-protein kinase 3) expression was significantly downregulated on the seventh postpartum day, consistent with loss of the cardiac regeneration potential in neonatal mice, and can promote cardiomyocyte proliferation and attenuate oxygen glucose deprivation/reoxygenation–induced cardiomyocyte apoptosis in vitro and ischemia/reperfusion injury–induced cardiomyocyte apoptosis in the infarct border zone in vivo.
- Overexpression of SGK3 in cardiomyocytes can promote cardiac regeneration and alleviate ischemia/reperfusion injury in mice.
- SGK3 regulates cardiac repair after apical resection and ischemia/reperfusion injury by regulating the GSK-3β (glycogen synthase kinase-3β)/β-catenin pathway.

What Are the Clinical Implications?

- We demonstrated that the SGK3 gene could regulate the process of cardiac regeneration after myocardial insult, providing a new therapeutic target for improving the cardiac function after myocardial insult in clinical practice.
- Cardiomyocyte-specific SGK3 overexpression-adenovirus serotype 5 (Ad5-cTNT-SGK3) and cardiomyocyte-specific SGK3 overexpression-adeno-associated virus serotype 9 (AAV9-cTNT-SGK3), 2 kinds of myocardium-specific overexpressed SGK3 vectors, have the potential to be used as gene therapy of myocardial insult.
- Local injection of SGK3 protein kinase via microcatheter in the area of myocardial infarction during interventional therapy may be a new therapeutic strategy to promote cardiac repair after myocardial infarction.

Nonstandard Abbreviations and Acronyms

AAV9	adeno-associated virus serotype 9
AKT	RAC-alpha serine/threonine-protein kinase
AKT1	RAC-alpha serine/threonine-protein kinase 1
AKT3	RAC-alpha serine/threonine-protein kinase 3
AR	apical resection
BIO	6-bromoindirubin-3'-oxime
CON	control
cTNT	cardiac troponin T
CST	cell signaling technology

cyclin D1	G1/S-specific cyclin-D1
GSK-3β	glycogen synthase kinase-3β
I/R	ischemia/reperfusion

cells.[2] Countless efforts have been made to prevent the loss of cardiomyocytes caused by ischemic heart disease.[3] Because of the low survival rate and low transformation efficiency of exogenous stem cells in the treatment of ischemic heart disease, exploring the molecular pathways capable of regulating the endogenous cardiomyocyte proliferation is expected to become the main approach for myocardial regeneration in the setting of ischemic heart disease in the future.[4] Reactivating key genes associated with the cardiac development to induce adult cardiomyocytes to reenter the cell cycle has recently become an attractive avenue.[5–7] Cell cycle regulatory genes, such as cell cycle dependent kinases and noncoding RNAs, which are temporarily overexpressed in the neonatal heart, can promote the adult cardiomyocyte proliferation if they are re-overexpressed in the adult heart.[7,8] Previously, we performed quantitative phosphoproteomic analysis to reveal the protein kinase network in the process of cardiac regeneration and elucidate the role of CHK1 (checkpoint kinase 1) in promoting cardiac regeneration.[6]

Intriguingly, several Hippo/Yap pathway kinases (eg, large tumor suppressor kinase 1 and 2) and RAC-alpha serine/threonine-protein kinase (AKT) pathway kinases (eg, RAC-alpha serine/threonine-protein kinase 1 [AKT1] and RAC-alpha serine/threonine-protein kinase 3 [AKT3] kinases) were marginally enriched (0.05<false discovery rate<0.1) in neonatal myocardial tissue at 6 days after infarction. Evidence has been reported that both Hippo/Yap and AKT pathways exert key regulatory roles in cardiac regeneration.[9–11] It remains unknown if these borderline enriched kinases after cardiac injury might also play key roles in the cardiac regeneration process. Through a series of screening and validation, SGK3 (serine/threonine-protein kinase 3), which is abundantly expressed in neonatal heart and borderline activated after MI in neonatal mice, attracted our attention.

SGK3 kinase, the key protein kinase screened from the marginal enriched kinases, belongs to the AGC-kinase (protein kinase A, G, and C) family and is highly conserved among species.[12] SGK3 and AKT kinases are homologous isomers, which are both downstream kinases of the phosphatidylinositol 3-kinase pathway and have the ability to recognize a host of identical downstream substrates.[13] AKT, as a key kinase in the regulation of cardiac injury repair, is known to be involved in the regulation of cardiac regeneration
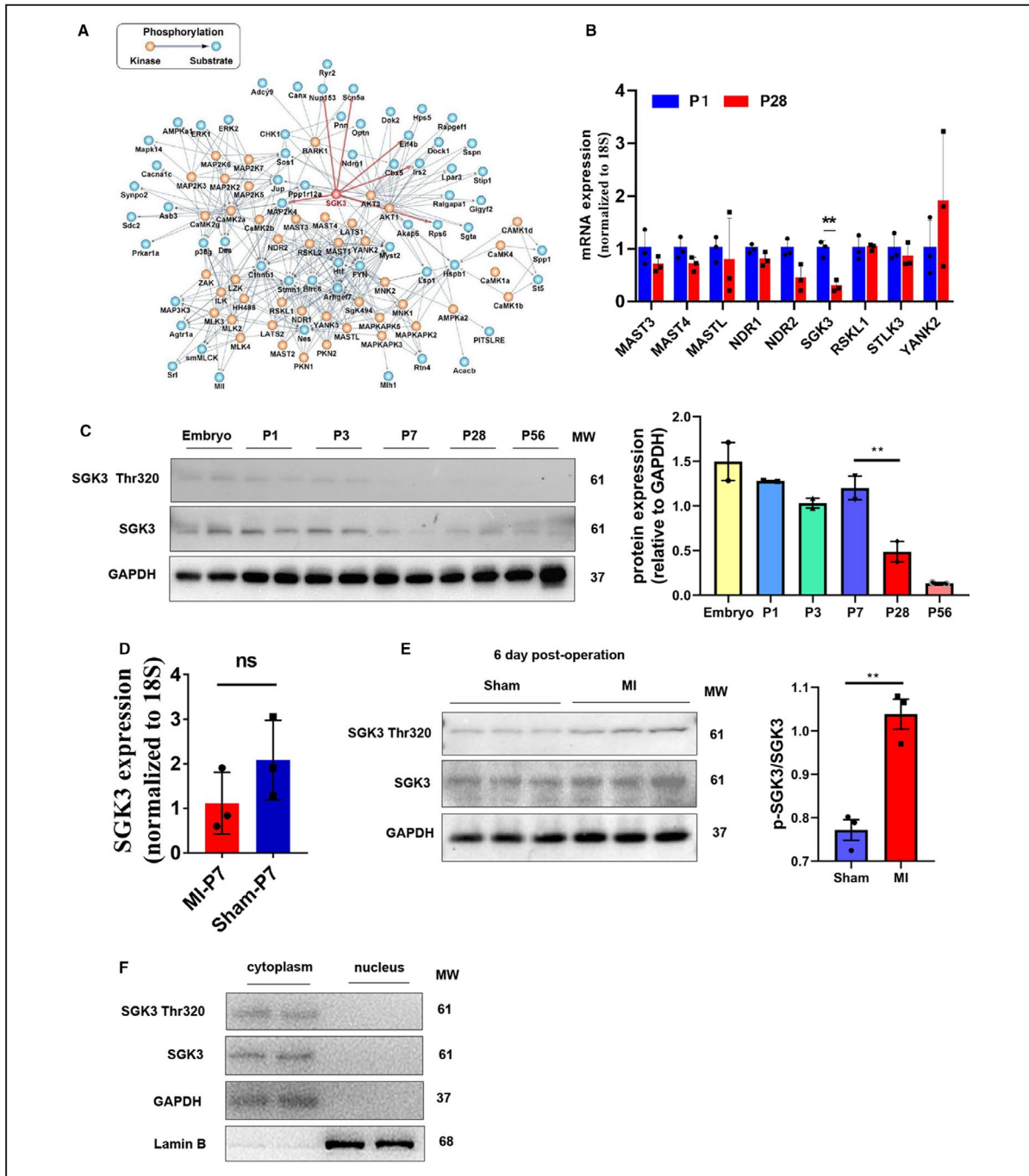
Figure 1.   Biological characteristics of SGK3 (serine/threonine-protein kinase 3) in the mouse heart.

A, The kinase-substrate network was constructed according to the proteins with upregulated phosphorylation levels (FDR ≤0.1). Blue dots mean substrates with upregulated phosphorylation levels identified in phosphoproteomics; yellow dots (including SGK3) indicate kinases with enriched upregulated substrate phosphorylation sites by iGPS; and the gray arrow links the kinase and its substrates. **B**, The mRNA expression of MAST3, MAST4, MASTL, NDR1, NDR2, SGK3, RSKL1, STLK3, and YANK2 in ventricular myocardium of P1 and P28 mice was detected by quantitative real-time polymerase chain reaction analysis (n=3). **C**, SGK3, phosphorylated (p) SGK3 Thr320 in mice ventricular myocardium from embryo to P56 were determined by Western blot. **D**, qRT-PCR analysis was used to detect the SGK3 expression in ventricular myocardium at P7 after myocardial infarction (MI) (n=3). **E**, SGK3, phosphorylated proteins of the Thr320 site in neonatal mice ventricular myocardium after MI were examined by Western blot. **F**, The subcellular localization of SGK3 in cardiomyocytes was evaluated by nuclear cytoplasmic separation and Western blot detection. Data are presented as mean±SEM. **$P<0.01$. 18S indicates 18S ribosomal DNA; FDR, false recovery rate; GAPDH, glyceraldehyde-3-phosphate dehydrogenase; MAST3, microtubule associated serine/threonine kinase 3; MAST3, microtubule associated serine/threonine kinase 3; MAST3, microtubule associated serine/threonine kinase 3; MAST3, microtubule associated serine/threonine kinase 3; MAST4, microtubule associated serine/threonine kinase 4; MASTL, microtubule associated serine/threonine kinase like; mRNA, messenger RNA; MW, molecular weigh; NDR1, nuclear Dbf2-related kinase 1; NDR2, nuclear Dbf2-related kinase 2; NS, no significance; P, postpartum day; RSKL1, ribosomal protein S6 kinase C1; STLK3, germinal centre kinase III; and YANK2, serine/threonine kinase 32B.

as a downstream target kinase of multiple genes.[11,14] Similarly, SGK3 kinase is involved in many biological processes, such as cell proliferation and survival, ion and protein transport, tumor malignant transformation, calcium and phosphorus absorption, and hair growth.[15–18] Here, we found that SGK3 expression was significantly downregulated at 7 days postpartum, which was consistent with the loss of cardiac
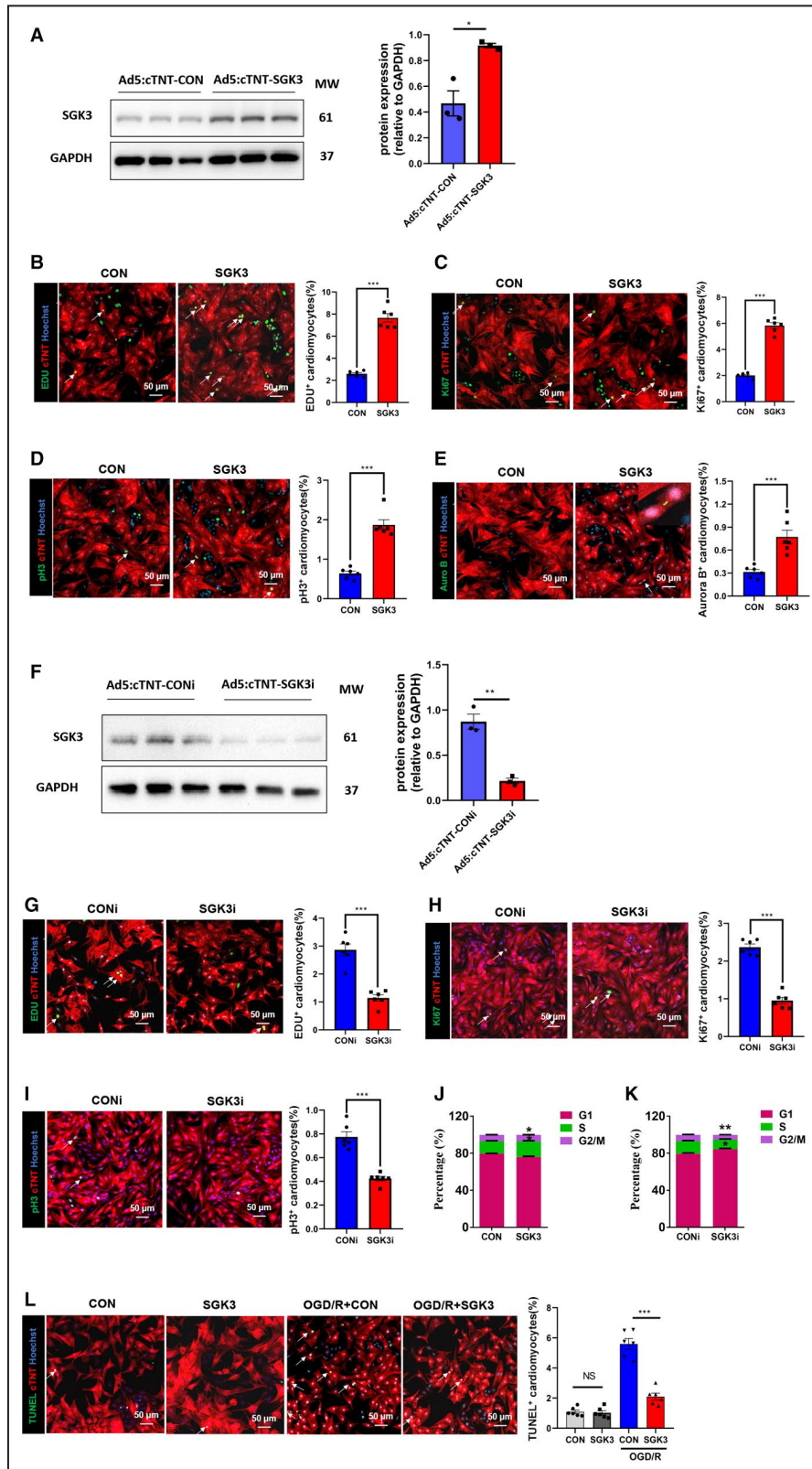
Figure 2. SGK3 (serine/threonine-protein kinase 3) regulates primary neonatal proliferation and apoptosis in vitro.

A, SGK3, phosphorylated (p-) proteins of SGK3 Thr320 in neonatal cardiomyocytes transfected with Ad5:cTNT-CON or Ad5:cTNT-SGK3 were detected by Western blot. **B** through **E**, cardiomyocytes isolated from 100 P1 mice were transfected with Ad5:cTNT-CON or Ad5:cTNT-SGK3, and immunofluorescence staining was then used to evaluate the cardiomyocyte proliferation for EDU+ (5639 cardiomyocytes in the Ad5:cTNT-SGK3 group and 5996 cardiomyocytes in the Ad5:cTNT-CON group, n=6 (**B**); Ki67+ (6511 cardiomyocytes in the Ad5:cTNT-SGK3 group and 6852 cardiomyocytes in the Ad5:cTNT-CON group, n=6 (**C**); pH3+ (8391 cardiomyocytes in the Ad5:SGK3 group and 7121 cardiomyocytes in the Ad5:cTNT-CON group, n=6 (**D**); and Aurora B+ (8503 cardiomyocytes in the Ad5:SGK3 group and 14 162 cardiomyocytes in the Ad5:cTNT-CON group, n=6 (**E**). **F**, SGK3 expression in neonatal cardiomyocytes transfected with Ad5:cTNT-SGK3i or Ad5:cTNT-CONi were analyzed by Western blot analysis. **G** through **I**, Immunofluorescence staining of cardiomyocytes isolated from 100 P1 mice transfected with Ad5:cTNT-SGK3i or Ad5:cTNT-CONi and quantification of EDU+ (4716 cardiomyocytes in the Ad5:SGK3i group and 4736 cardiomyocytes in the Ad5:cTNT-CONi group, n=6 (**G**); Ki67+ (6388 cardiomyocytes in the Ad5:cTNT-SGK3i group and 9583 cardiomyocytes in the Ad5:cTNT-CONi group, n=6 (**H**); and pH3+ (5642 cardiomyocytes in the Ad5:cTNT-SGK3i group and 6576 cardiomyocytes in the Ad5:cTNT-CONi group, n=6 (**I**). **J** and **K**, Cell flow cytometry was performed to detect the cell cycle of cardiomyocytes after SGK3 overexpression or inhibition. **L**, Terminal deoxynucleotidyl transferase-mediated dUTP in situ nick end labeling (TUNEL) staining was performed to evaluate the effect of Ad5:cTNT-SGK3 on oxygen glucose deprivation/reoxygenation (OGD/R)-induced neonatal mouse cardiomyocyte apoptosis (3657 cardiomyocytes in the Ad5:cTNT-CON group, 3017 cardiomyocytes in the Ad5:cTNT-SGK3 group, 2049 cardiomyocytes in the OGD/R+Ad5:cTNT-CONi group, and 1303 cardiomyocytes in the OGD/R+Ad5:cTNT-SGK3 group, n=6). The cells indicated by the arrows are immunofluorescence-positive cardiomyocytes. Data are presented as mean±SEM. *$P \leq 0.05$; **$P \leq 0.01$; ***$P \leq 0.001$. Ad5:cTNT-CON indicates control adenovirus serotype 5; Ad5:cTNT-CONi, knockdown control adenovirus serotype 5; Ad5:cTNT-SGK3, cardiomyocyte-specific SGK3 overexpression adenovirus serotype 5; Ad5:cTNT-SGK3i, cardiomyocyte-specific SGK3 knockdown adenovirus serotype 5; CON, control; CONi, knockdown control; cTNT, cardiac troponin T; EDU, 5-ethynyl-2′-deoxyuridine; G1, G1 phase; G2/M, G2/M phase; GAPDH, glyceraldehyde-3-phosphate dehydrogenase; ki67+, ki67 positive; NS, no significance; P1, postpartum day 1; ph3+:phospho-histone H3 positive; S, S phase; and SGK3i, serine/threonine-protein kinase 3 knockdown.

regeneration capacity, and could be activated after MI injury in neonatal mice. In addition, many core genes capable of promoting cardiac regeneration, such as GSK-3β (glycogen synthase kinase-3β)/β-catenin, G1/S-specific cyclin-D1 (cyclin D1), and mechanistic target of rapamycin kinase (mTOR), have been reported to be regulated by SGK3 in previous studies.[15,19,20] However, the functional role of SGK3 in cardiac regeneration and whether SGK3 can promote cardiac regeneration by regulating regenerative core genes remain elusive now.

In this study, we identified that SGK3 was significantly downregulated in myocardium beginning from postnatal day 7 to adulthood. SGK3 overexpression in the infarct border myocardial tissues resulted in markedly augmented myocardial repair and improved cardiac function after I/R injury, suggesting a regenerative and cardioprotective role of SGK3 after I/R injury.

METHODS

The data that support the findings of this study are available from the corresponding author on request. The raw data related to phosphorylation proteomics are uploaded to the ProteomeXchange Consortium.[6] Additional methods can be found in Data S1.

Availability of Data and Material

All data generated or analyzed during this study are included in this article.

Ethical Statement

All animal studies were approved by the Institutional Animal Care and Use Committee of Nanjing Medical University and conformed to the Guide for the Care and Use of Laboratory Animals published by the US National Institutes of Health (publication no. 85-23, revised 1996).

Experimental Animals

All animal experiments were performed in accordance with the *Guide for the Use and Care of Laboratory Animals* and approved by Animal Care and Use Committee of Nanjing Medical University. Wild-type Institute of Cancer Research mice were obtained from the animal center of Nanjing Medical University and reared in a specific pathogen-free environment.

RNA Extraction and Quantitative Real-Time Polymerase Chain Reaction Analysis

Total RNA from the myocardial tissue used in our study was extracted with TRIzol reagent (Thermo Fisher Scientific) according the manufacturer's instructions. The PrimeScript RT Master Mix kit (Takara Bio, Kusatsu, Japan) was used to synthesize complementary DNA. Relative RNA levels analysis, detected by quantitative real-time polymerase chain reaction analysis, was performed on a Roche Lightcycler 96 by using the SYBR Green (Vazyme Biotech, Nanjing, China; Q131-02). 18S ribosomal DNA was used as an internal control, and determined genes sequences for quantitative real-time polymerase chain reaction analysis primers in this study are shown in Table S1.

Western Blot Analysis

Myocardial tissues or cardiomyocytes were lysed with lysis buffer (including 0.5% phenylmethylsulfonyl

fluoride, 0.1% protease inhibitor, and 1% phosphatase inhibitor) (Genechem, Shanghai, China). Prepared protein was separated in SDS-PAGE gels, transferred onto a polyvinylidene fluoride membrane (Millipore), and blocked with 5% bovine serum albumin. The strips were incubated with primary antibodies overnight at 4 °C. Specific primary antibody information is as follows:

anti-SGK3 (cell signaling technology [CST]; 8573S), anti-phospho-SGK3 (Thr320) (CST; 5642S), anti-GSK-3β (CST; 12456T), anti-phospho-GSK-3β (CST; 5558T), anti-β-catenin (CST; 8480S), anti-mTOR (CST; 2983S), anti-phospho-mTOR (S2448) (CST; 5536S), and anti-glyceraldehyde-3-phosphate dehydrogenase (CST; 5174S). Then, the blots were cultured with the
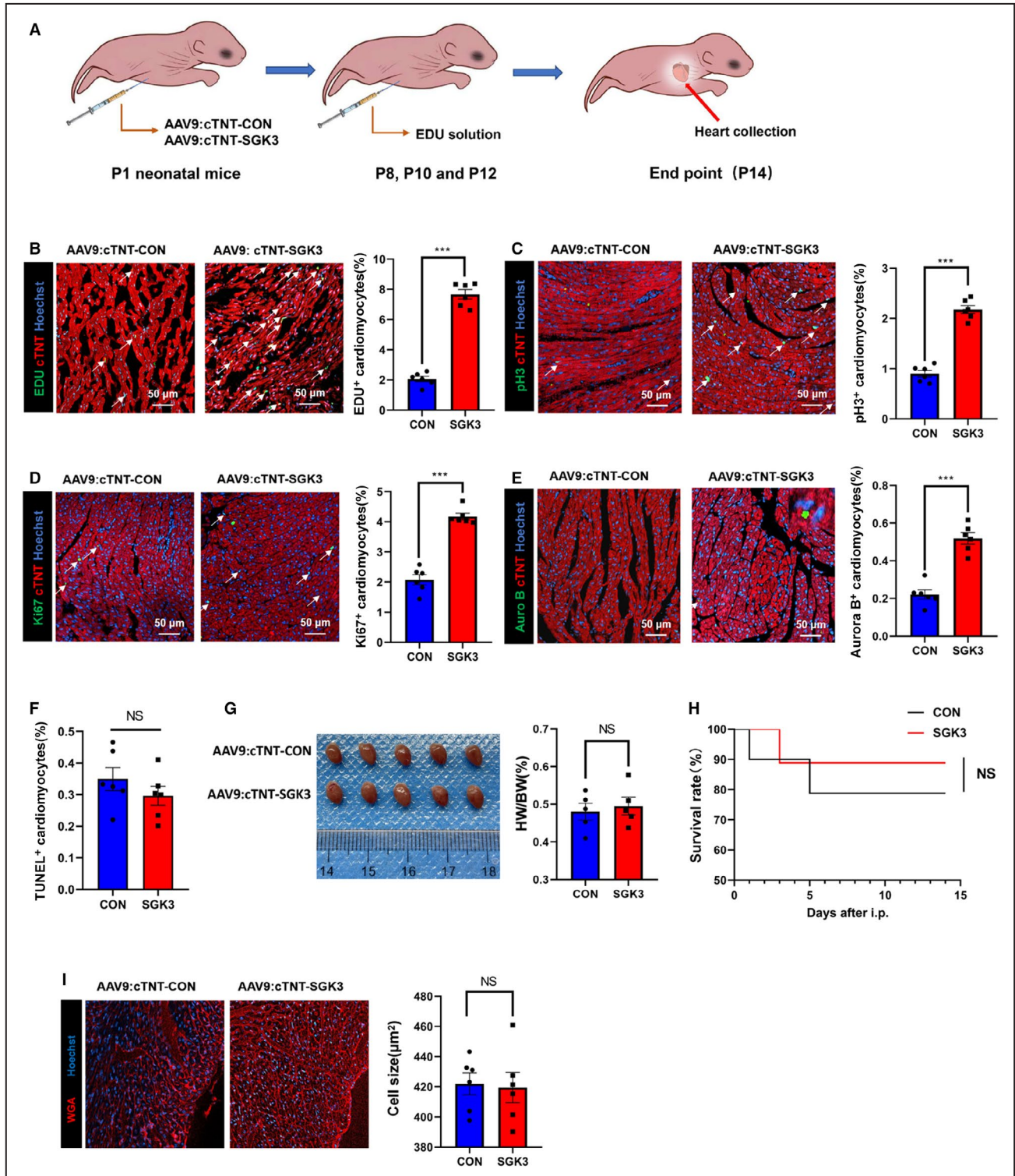
Figure 3. SGK3 (serine/threonine-protein kinase 3) overexpression enhances neonatal cardiomyocyte proliferation in vivo.
A, Experimental pattern: myocardium targeting SGK3 overexpression of adeno-associated virus serotype 9 (AAV9:cTNT-SGK3) or control (AAV9:cTNT-CON) was intraperitoneally injected into P1 mice, and intraperitoneally injected EDU solution at P8, P10, and P12, and the hearts were then collected at P14 for relevant experiments. **B** through **E**, After 14 days treatment of AAV9:cTNT-SGK3 or AAV9:cTNT-CON in P1 mice, immunofluorescence staining was then performed at P14 to evaluate the cardiomyocyte proliferation for EDU[+] (12 565 cardiomyocytes in the AAV9:cTNT-SGK3 group and 12 678 cardiomyocytes in the AAV9:cTNT-CON group, n=6 (**B**); pH3[+] (10 067 cardiomyocytes in the AAV9:cTNT-SGK3 group and 5788 cardiomyocytes in the AAV9:cTNT-CON group, n=6 (**C**); Ki67^{+} (9908 cardiomyocytes in the AAV9:cTNT-SGK3 group and 10 241 cardiomyocytes in the AAV9:cTNT-CON group, n=6 (**D**); and Aurora B[+] (18 132 cardiomyocytes in the AAV9:cTNT-SGK3 group and 17 707 cardiomyocytes in the AAV9:cTNT-CON group, n=6 (**E**). **F**, Terminal deoxynucleotidyl transferase-mediated dUTP in situ nick end labeling (TUNEL) staining was used to evaluate the effect of AAV9:cTNT-SGK3 or AAV9:CTNT-CON on cardiomyocyte apoptosis in mice at P14 (5723 cardiomyocytes in the AAV9:cTNT-SGK3 group and 5457 cardiomyocytes in the AAV9:cTNT-CON group, n=6). **G**, Heart weight/body weight (HW/BW) ratio and cardiac morphology between AAV9:cTNT-SGK3 (n=5) and AAV9:cTNT-CON mice (n=5) at P14. **H**, Survival rate was analyzed by between AAV9:cTNT-CON (n=10) and AAV9:cTNT-SGK3 (n=10). **I**, Wheat germ agglutinin (WGA) immunofluorescence was used to detect the cardiomyocyte size between AAV9:cTNT-SGK3 and AAV9:cTNT-CON mice at P14 (14 687 cardiomyocytes in the AAV9:cTNT-SGK3 group and 14 582 cardiomyocytes in the AAV9:cTNT-CON group, n=6). Data are presented as mean±SEM. ***$P \leq 0.001$. CON indicates control; cTNT, cardiac troponin T; EDU, 5-ethynyl-2′-deoxyuridine; i.p., intraperitoneal; ki67+, ki67 positive; NS, no significance; P1, postpartum day 1; P14, postnatal day 14; and pH3+, phospho-histone H3 positive.

second antibody conjugated to horseradish peroxidase at room temperature for 2 hours. Quantification of band intensity was performed using Image J software (National Institutes of Health, Bethesda, MD).

Immunofluorescence Staining

Hearts were harvested and fixed overnight in 4% paraformaldehyde and then embedded in paraffin. Paraffin-embedded hearts were cut into 5-μm tissue sections and boiled in antigen retrieval buffer (BD Pharmingen) for 10 minutes. Then, the sections were immersed in PBS containing 0.2% Triton X-100 for 15 minutes and blocked with 5% bovine serum albumin for 2 hours. To identify cell-cycle activities and cytokinesis, the Click-iT EdU Imaging Kits (Thermo Fisher), anti-Ki67 antibody (Abcam; ab16667), anti-Aurora B antibody (Abcam; ab2254), and anti-phosphorylated-histone 3 (pH3) antibodies (CST; 9701) were used to culture sections and formaldehyde-fixed cardiomyocytes. Terminal deoxynucleotidyl transferase-mediated dUTP in situ nick end labeling (TUNEL) staining was performed to determine the cardiomyocyte apoptosis in vivo. WGA (wheat germ agglutinin) staining (Thermo Fisher; w32466) was performed to stain the cell membrane, anti-cardiac troponin T (cTNT) (Abcam; ab8295) was used to label cardiomyocytes, and N-acetyl-diaminopimelate deacetylase was used to mark nuclei. Quantitative data were obtained by measuring confocal microscope (Zeiss, Oberkochen, Germany).

In vitro, neonatal mouse cardiomyocytes were cultured in 24-well plates. After being treated with different adenoviruses or reagents, the nonadherent cells were washed out with PBS, and the adherent cardiomyocytes were then fixed with 4% paraformaldehyde for 20 minutes. After being sealed with 10% goat serum for 1 hour, 5-ethynyl-2′-deoxyuridine (EDU), Ki67, pH3, WGA, and TUNEL staining were performed. Finally, a Zeiss microscope (Carl Zeiss Microscopy, Jena, Germany) was used to take pictures and count the randomly selected visual field. The statistical data of all immunofluorescence staining in this study are shown in Table S2.

Statistical Analysis

All the statistical data were analyzed using SPSS 22.0 (IBM, Armonk, USA) and were presented as mean±SEM using GraphPad (La Jolla, CA) Prism 8.0 software. For the comparison of mean values between 2 groups, an unpaired Student t test was performed when the data were shown to be normally distributed. For the comparisons among multiple groups, 1-way ANOVA (with the Tukey multiple comparisons test) was performed to determine the statistical differences. A log-rank (Mantel-Cox) test was performed to analyze the survival rate. Differences were considered statistically significant when $P \leq 0.05$.

RESULTS

SGK3 Is Upregulated After MI in the Neonatal Heart

pH3-positive cell staining confirmed that the cardiomyocyte proliferation ability was significantly decreased in P7 and P28 hearts compared with the P1 heart, which was consistent with the lost regeneration capacity of mammalians at P7 (Figure S1). Quantitative proteomic analysis of protein and phosphorylation level in infarct margin myocardial tissue of P1 MI mice at 6 days after infarction was performed in our previous study. Besides 11 activated kinases (false discovery rate ≤ 0.05),[6] several borderline enrichment kinases, which belong to Hippo/Yap pathway kinases (eg, large tumor suppressor kinase 1 and 2) and AKT signaling kinases (eg, AKT1 and AKT3) were defined at 6 days after infarction of P1 MI mice (0.05 < false discovery rate < 0.1) (Figure 1A and Table S3).

To explore the potential role of these marginally enriched kinases on cardiac regeneration, we screened
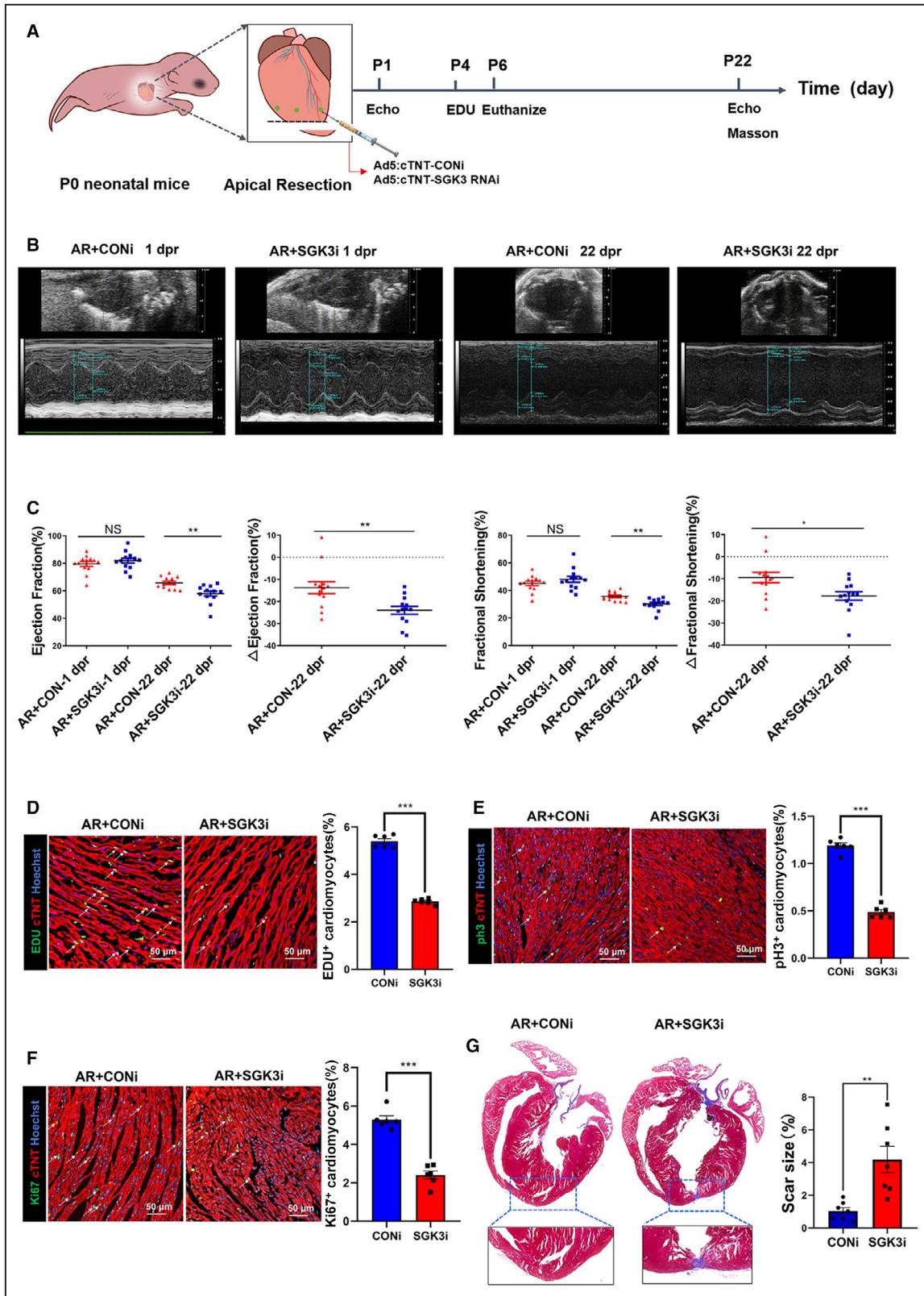
9 out of the 35 marginally enriched protein kinases that could mediate cell proliferation but were not reported in cardiovascular field, and detected their mRNA levels using quantitative real-time polymerase chain reaction analysis in neonatal (P1) and adult (P28) myocardial tissue. Results indicated that mRNA expression of SGK3 (one of the borderline enrichment kinases; $P=0.0039$, false discovery rate=0.0632), was significantly

Figure 4. SGK3 (serine/threonine-protein kinase 3) inhibition impairs neonatal cardiac regeneration after apical resection.
A, Experimental pattern: adenovirus serotype 5 SGK3i (Ad5:cTNT-SGK3i) or control (Ad5:cTNT-CONi) was injected into border myocardium after apical resection (AR) in P1 mice using microinjector. EDU solution was then intraperitoneally injected at 4 days post resection (dpr). Finally, the cardiomyocyte proliferation was detected at 6 dpr, and cardiac function was evaluated at 22 dpr. **B** and **C**, Cardiac function of ejection fraction and fractional shortening between Ad5:cTNT-SGK3i or Ad5:cTNT-CONi treated mice at 1 and 22 days after AR (Ad5:cTNT-SGK3i group, n=13; Ad5:cTNT-CONi, n=13). **D** through **F**, Immunofluorescence staining was used to evaluate the cardiomyocyte proliferation between Ad5:cTNT-SGK3i– or Ad5:cTNT-CONi–treated mice at P6 for EDU$^+$ (11 873 cardiomyocytes in the Ad5:cTNT-SGK3i group and 11 755 cardiomyocytes in the Ad5:cTNT-CON group, n=6 (**B**); pH3$^+$ (15 210 cardiomyocytes in the Ad5:cTNT-SGK3i group and 15 084 cardiomyocytes in the Ad5:cTNT-CON group, n=6(**C**); and Ki67$^+$ (12 290 cardiomyocytes in the Ad5:cTNT-SGK3i group and 13 119 cardiomyocytes in the Ad5:cTNT-CON group, n=6 (**D**). **G**, Masson staining of mouse ventricular cross-sections between Ad5:cTNT-SGK3i– or Ad5:cTNT-CONi–treated mice at 22 days after AR (n=7 in each group). Data are presented as mean±SEM. *$P \le 0.05$; **$P \le 0.01$; ***$P \le 0.001$. CON indicates control; CONi, knockdown control; cTNT, cardiac troponin T; EDU, 5-ethynyl-2′-deoxyuridine; ki67+, ki67 positive; NS, no significance; P1, postpartum day 1; and pH3+, phospho-histone H3 positive.

downregulated in P28 myocardial tissues than that in P1 mice (Figure 1B). Total protein and phosphorylation levels of SGK3 were also decreased remarkably in the heart of P7 mice as compared with that in P1 mice (Figure 1C). Additionally, the mRNA expression of SGK3 did not change significantly (Figure 1D), but the phosphorylated-SGK3/SGK3 ratio was elevated significantly after MI in neonatal mice ($P=0.0031$; Figure 1E). Nuclear cytoplasmic separation experiments and Western blot analysis revealed that SGK3 mainly existed in the cytoplasm (Figure 1F). Finally, conservative analysis showed high homology of SGK3 gene between human and mouse (Figure S2).

SGK3 Mediates Primary Neonatal Cardiomyocyte Proliferation In Vitro

Given that the time of SGK3 protein expression decrease is coincident with the time of the decreased regenerative capacity in neonatal mice, we tested if SGK3 could mediate the cardiomyocyte proliferation. We first transfected cardiomyocytes with different titers (multiplicity of infection=10, 25, 50, and 100) of cardiomyocyte-specific SGK3 overexpression associated adenovirus vector 5 (Ad5:cTNT-SGK3) or SGK3 knockdown-associated adenovirus vector 5 (Ad5:cTNT-SGK3i) for 48 hours, and selected multiplicity of infection=50 as the most appropriate transfection titer according to the fluorescence intensity (Figure S3A and S3B). Western blot analysis results revealed that the SGK3 protein levels in P1 neonatal cardiomyocytes was markedly elevated at 48 hours after Ad5:cTNT-SGK3 transfection ($P=0.0103$; Figure 2A). Immunofluorescence staining indicated that SGK3 overexpression promoted cardiomyocyte proliferation, as characterized by the increase of DNA synthesis (EDU$^+$: control [CON]: 2.595±0.104%, SGK3: 7.66±0.38%; $P<0.0001$), cell cycle activity (Ki67$^+$: CON: 2.01±0.07381%, SGK3: 5.832±0.2178%; $P<0.0001$), and mitotic (pH3$^+$: CON: 0.6392±0.05629%, SGK3: 1.869±0.1304%; $P<0.0001$) of primary neonatal cardiomyocytes (Figure 2B through 2D). We also used Aurora B, which is commonly considered to be a

cytokinesis marker. The results are consistent with the interpretation that overexpression of SGK3 significantly promoted the cytokinesis of cardiomyocytes (Aurora B$^+$: CON: 0.3139±0.03186%, SGK3: 0.7722±0.08794%; $P=0.0006$) (Figure 2E), but we did not present direct evidence of cell division in our work; this point should be kept in mind when interpreting our findings. Next, to explore whether SGK3 inhibition could reduce neonatal cardiomyocyte proliferation, cardiomyocyte-specific SGK3 knockdown adenovirus vector (Ad5:cTNT-SGK3i, multiplicity of infection=50) or knockdown control adenovirus serotype 5 (Ad5:cTNT-CONi, multiplicity of infection=50) was transfected into primary neonatal cardiomyocytes for 48 hours. Protein expression of SGK3 was significantly decreased in Ad5:cTNT-SGK3i transfected cardiomyocytes compare with that in Ad5:cTNT-CONi cardiomyocytes ($P=0.0018$; Figure 2F). As expected, the ratio of cell proliferation (EDU$^+$: CON: 2.869±0.2059%, SGK3: 1.142±0.1124%; $P<0.0001$; Ki67$^+$: CON: 2.37±0.08264%, SGK3: 0.9532±0.08455%; $P<0.0001$; and pH3$^+$: CON: 0.7745±0.04332%, SGK3: 0.4237±0.01922%; $P<0.0001$) was significantly reduced in Ad5:cTNT-SGK3i– transfected primary neonatal cardiomyocytes (Figure 2G through 2I). Consistent with the above results, cell flow cytometry results showed that SGK3 overexpression significantly increased, whereas SGK3 inhibition remarkably inhibited the proportion of cardiomyocytes in DNA synthesis and mitotic state (Figure 2J and 2K). Moreover, the level of cardiac fibroblast proliferation (Ki67$^+$) was not affected by Ad5:cTNT-SGK3 ($P=0.476$) and Ad5:cTNT-SGK3i ($P=0.479$) (Figure S3C and S3D). Finally, to verify the effect of SGK3 on cardiomyocyte apoptosis after I/R injury, we established an in vitro model of oxygen glucose deprivation/reoxygenation using an AnaeroPACK Rectangular Jar. After 24 hours of Ad5:cTNT-SGK3 transfection, cardiomyocytes were incubated in glucose and serum-free media for 8 hours in the AnaeroPACK Rectangular Jar at 37 °C, and then reoxygenated in DMEM medium containing glucose for 12 hours. TUNEL immunofluorescence assay (CON: 5.587±0.3628%, SGK3: 2.097±0.2237%;

P<0.0001) showed that SGK3 did not affect the apoptosis rate of neonatal cardiomyocytes under physiological conditions, but could significantly reduce the apoptosis rate of cardiomyocytes induced by oxygen glucose deprivation/reoxygenation (Figure 2L).

SGK3 Overexpression Enhances Cardiomyocyte Proliferation in Neonatal Mice

To identify the effects of SGK3 on the proliferation, apoptosis, heart weight/body weight ratio, and
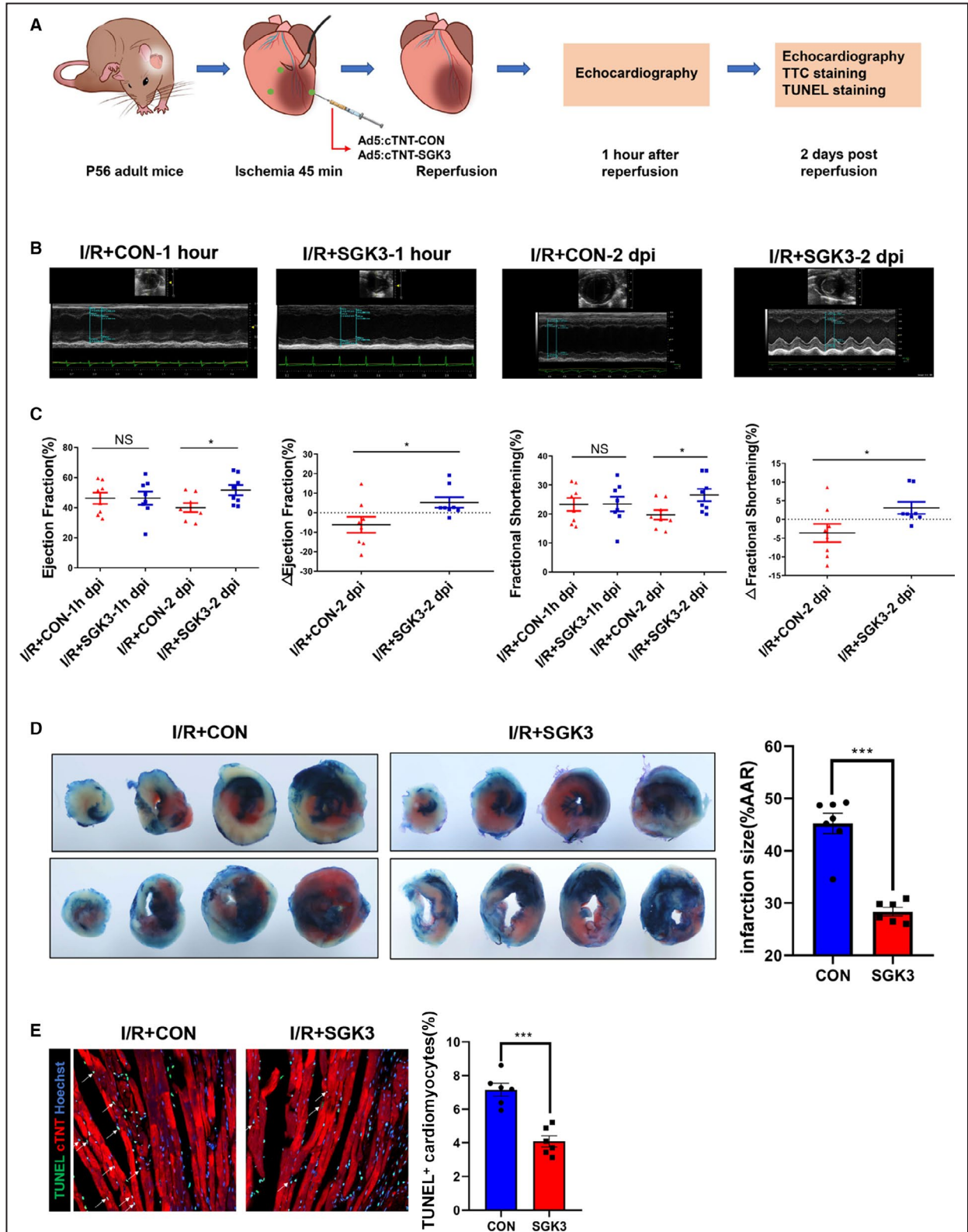
Figure 5. SGK3 (serine/threonine-protein kinase 3) overexpression improved cardiac repair in acute stage after ischemia/reperfusion (I/R) injury.

A, Experimental pattern: myocardium targeting SGK3 overexpression of Ad5:cTNT-SGK3 or Ad5:cTNT-CON was injected into infarct border myocardium after ischemia. After 45 minutes of ischemia, the ligation line was released for reperfusion, and then echocardiography or TTC staining were performed, respectively, at 1 and 48 hours after operation. **B** and **C**, Cardiac function of ejection fraction and fractional shortening between Ad5:cTNT-SGK3–(n=8) or Ad5:cTNT-CON–treated mice at 1 and 48 hours after I/R injury (n=8). **D**, TTC staining of mouse ventricular cross-sections between Ad5:cTNT-SGK3 (n=6) or Ad5:cTNT-CON mice at 48 hours after I/R injury (n=7). **E**, Terminal deoxynucleotidyl transferase-mediated dUTP in situ nick end labeling (TUNEL) immunofluorescence staining was then performed to evaluate the cardiomyocyte apoptosis (2577 cardiomyocytes in infarction border zone Ad5:cTNT-CON group, 2222 cardiomyocytes in the infarction border zone of AAV9:cTNT-SGK3 group, n=6). Data are presented as mean±SEM. $*P\leq0.05$; $***P\leq0.001$. AAR indicates area at risk; Ad5:cTNT-CON, control adenovirus serotype 5; Ad5:cTNT-SGK3, cardiomyocyte-specific SGK3 overexpression adenovirus serotype 5; CON, control; dpi, days post infarction; NS, no significance; P56, postpartum day 56; and TTC, 2,3,5-Triphenyltetrazolium chloride.

cardiomyocyte size in neonatal mice without heart injury, adeno-associated virus serotype 9 (AAV9):cTNT-SGK3 (1.1×10^{12} vg/mL, total stock solution volume=8 µL/mouse) or AAV9:cTNT-CON (1.1×10^{12} vg/mL, total stock solution volume=8 µL/mouse) were intraperitoneally injected into P1 mice, and EDU solution (5 µg/µL, total volume=70 µL) was then injected at different time points (details shown in Figure 3A). The transfection efficiency of AAV9:cTNT-SGK3 was confirmed by an elevated expression of SGK3 in ventricular myocardium of neonatal mice by Western blot analysis (Figure S4). Immunofluorescence staining results indicated that overexpression of SGK3 promoted the ratio of cell proliferation, as represented by the increase of EDU$^+$ (CON: 2.059±0.1782%, SGK3: 7.661±0.3192%; $P<0.0001$), pH3$^+$ (CON: 0.8998±0.06587%, SGK3: 2.176±0.08008%; $P<0.0001$), Ki67$^+$ (CON: 2.076±0.1674%, SGK3: 4.175±0.1074%; $P<0.0001$), and Aurora B$^+$ (CON: 0.2209±0.02458%, SGK3: 0.5191±0.02982%; $P<0.0001$) cardiomyocytes from ventricular tissue of postnatal day 14 mice (Figure 3B through 3E). Nevertheless, SGK3 overexpression did not affect the cardiomyocyte apoptosis (CON: 0.3495±0.03661%, SGK3: 0.2964±0.03%; $P=0.2879$), heart weight/body weight ratio (CON: 0.4801±0.02239%, SGK3: 0.4953±0.0238%; $P=0.6532$), survival rate and cardiomyocyte size (CON: 422±7.232, SGK3: 419.5±9.968; $P=0.8439$) of postnatal day 14 mice under physiological conditions (Figure 3F through 3I).

Inhibition of SGK3 Prevents Neonatal Cardiac Regeneration Following Apical Resection

In view of the robust regeneration ability of neonatal heart after cardiac injury, we explored whether SGK3 inhibition in resection border myocardium of neonatal mice could impair cardiomyocyte regeneration and cardiac repair capacity after apical resection (AR). Ad5:cTNT-SGK3i (2×10^{10} plaque forming unit/mL, total stock solution volume=0.5 µL/mouse, diluted to 6 µL with PBS) or Ad5:cTNT-CONi (1×10^{11} plaque forming unit/mL, total stock solution volume=0.1 µL/mouse, diluted to 6 µL with PBS) were injected into

3 different locations around the apex (2 µL for each point) after AR in P1 mice using a microinjector. EDU solution (5 µg/µL, total volume=70 µL/mouse) was then intraperitoneally injected at 4 days after resection (details shown in Figure 4A). Echocardiography results indicated that ejection fraction (CON: 58±1.8%, SGK3i: 65.8±1.2%; $P=0.0013$) and fractional shortening (CON: 30.2±1.1%, SGK3i: 35.7±0.9%; $P=0.001$) were significantly decreased at 22 days after resection in the SGK3 inhibition group than in the control group (Figure 4B and 4C). Hearts were also harvested at 6 days after resection and SGK3 protein expression, and proliferation markers were detected. Western blot analysis results showed that SGK3 expression was significantly decreased in the Ad5:cTNT-SGK3i group than that in the Ad5:cTNT-CONi group (Figure S5). A significant decrease of EDU$^+$ (CON: 5.398±0.1086%, SGK3: 2.863±0.04757%; $P<0.0001$), pH3$^+$ (CON: 1.191±0.02913%, SGK3: 0.486±0.02662%; $P<0.0001$), and Ki67$^+$ (CON: 4.7±0.1294%, SGK3: 1.914±0.1028%; $P<0.0001$) cardiomyocytes was also observed in resection border myocardium of Ad5:cTNT-SGK3i–treated mice compared with Ad5:cTNT-CONi–treated mice (Figure 4D through 4F). Finally, the Masson trichrome staining of heart cross-sections at 22 days after resection showed that the cardiac fibrosis rate after AR was significantly higher in Ad5:cTNT-SGK3i– treated mice (4.2±0.8%) than that in Ad5:cTNT-CONi–treated mice (1.0±0.2%, $P=0.0028$) (Figure 4G). These data show SGK3 silencing could abolish the heart regeneration and cardiac function recovery after AR injury in neonatal mice.

Overexpressing SGK3 Improves Myocardium Repair and Cardiac Function Recovery After I/R Injury in Adult Mice

To explore the acute effect of SGK3 on heart repair and cardiac function recovering in acute stage of I/R injury, adenovirus vector 5, which is effective 12 to 24 hours after injection and maximal efficacy observed at 48 to 96 hours after injection, was used. The Ad5:cTNT-SGK3 (2×10^{10} plaque forming unit/mL, total stock solution volume=5 µL/mouse, diluted to 9 µL

with PBS) or control adenovirus serotype 5 (Ad5:cTNT-CON: 1×10^{11} plaque forming unit/mL, total stock solution volume=1 µL/mouse, diluted to 9 µL with PBS)

were injected into 3 different locations around the apex (3 µL for each point) after I/R injury in P56 mice (details shown in Figure 5A). After 45 minutes of left anterior
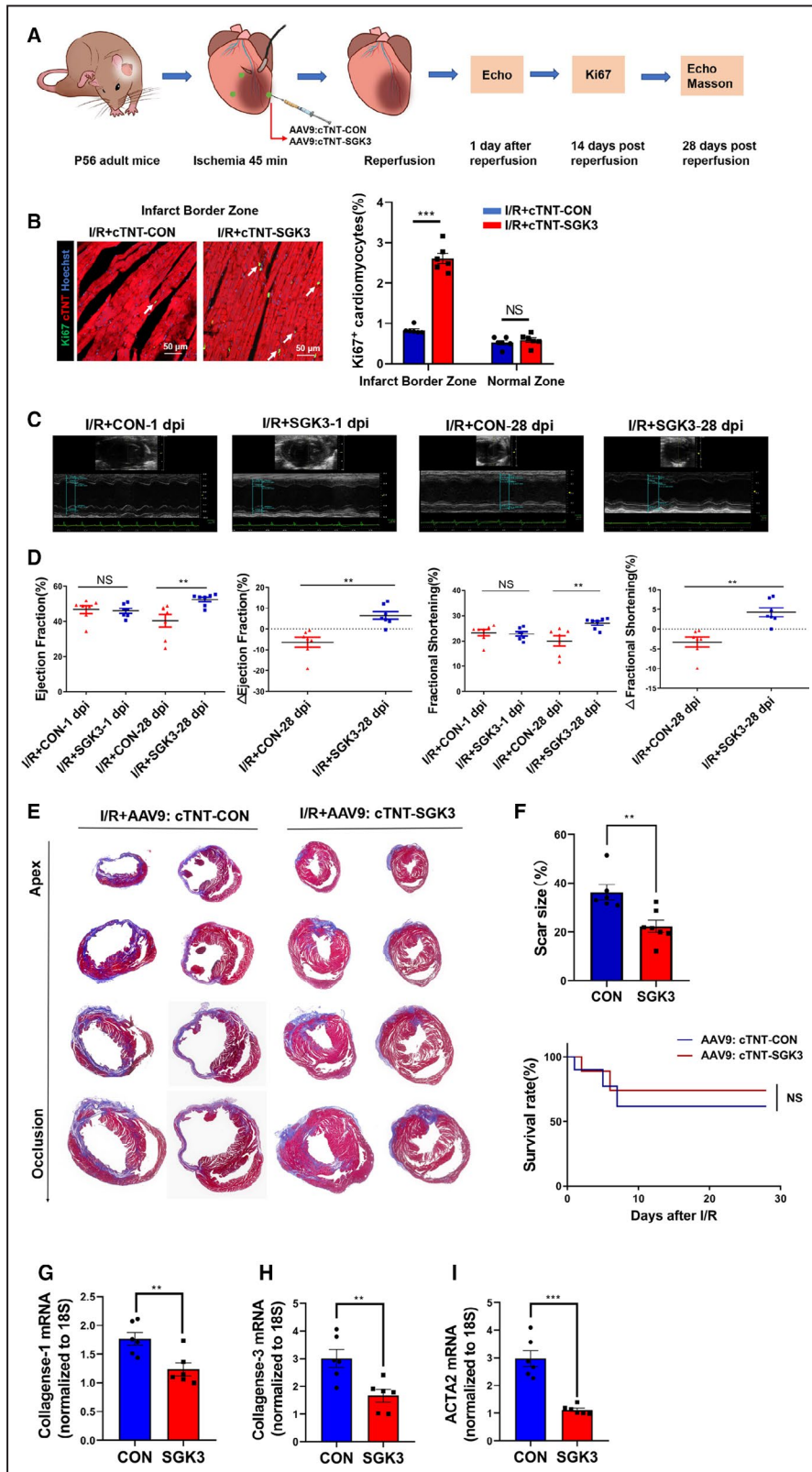
Figure 6. SGK3 (serine/threonine-protein kinase 3) overexpression ameliorates long-term improvement of cardiac function after ischemia/reperfusion I/R injury.

A, Experimental pattern: myocardium targeting SGK3 overexpression of AAV9:cTNT-SGK3 or AAV9:cTNT-CON was injected into infarct border myocardium after ischemia. After 45 minutes of ischemia, the ligation line was released for reperfusion, and then echocardiography or Masson staining were performed, respectively, at 1 and 28 days after I/R injury. **B**, Immunofluorescence staining was used to evaluate the cardiomyocyte proliferation between AAV9:cTNT-SGK3– or AAV9:cTNT-CON–treated mice at 14 days after I/R injury for Ki67+ (4157 in the infarct border zone of AAV9:cTNT-SGK3 group, 3264 cardiomyocytes in the normal zone of AAV9:cTNT-SGK3 group, 3734 cardiomyocytes in the infarct border zone of AAV9:cTNT-CON group, 3657 cardiomyocytes in the normal zone of AAV9:cTNT-CON group). **C** and **D**, Cardiac function of ejection fraction and fractional shortening between AAV9:cTNT-SGK3– (n=7) or AAV9:cTNT-CON–treated mice at 1 and 28 days after I/R injury (n=7). **E** and **F**, Masson staining of mouse ventricular cross-sections was performed to determine the scar size between AAV9:cTNT-SGK3 (n=7) and AAV9:cTNT-CON mice at 28-days after I/R (n=6). **G** through **I**, The fibrosis markers of Col-1, Col-2, and ACTA2 (actin alpha 2) in the infarction zone between the AAV9:cTNT-SGK3 and AAV9:cTNT-CON group were detected by quantitative real-time polymerase chain reaction RT-qPCR. **J**, The survival rate was quantified in adult mice at 28 days post infarction (dpi) between AAV9:cTNT-SGK3 (n=10) or AAV9:cTNT-CON groups (n=10). Data are presented as mean±SEM. **$P \leq 0.01$; ***$P \leq 0.001$. 18S indicates 18S ribosomal DNA; AAV9:cTNT-CON, control adeno-associated virus serotype 9; AAV9-cTNT-SGK3, cardiomyocyte-specific SGK3 overexpression-adeno-associated virus serotype 9; Col, collagense; CON, control; mRNA, messenger RNA; and NS, no significance.

descending coronary artery ligation, the suture was untied to allow reperfusion. Echocardiography was performed at 60 minutes and 48 hours after reperfusion, and ejection fraction (EF) (2 days after infarction EF: CON: 40.1±3.0%, SGK3: 51.6±3.4%; $P=0.022$) and fractional shortening (FS) (2 days after infarction FS: CON: 19.7±1.7%, SGK3: 26.6±2.1%; $P=0.023$) values were significantly higher after SGK3 overexpression (Figure 5B and 5C). After 2 days of I/R injury, the protein expression of SGK3 was significantly increased in infarct border myocardium, indicating the successful transfection of Ad5:cTNT-SGK3 in myocardial tissue (Figure S6A). The 2,3,5-Triphenyltetrazolium chloride and TUNEL staining were then performed to evaluate the effect of SGK3 in cardiac injury. Transfection of Ad5:cTNT-SGK3 robustly reduced the I/R injury–induced infarct size/area at risk (infarction area/area at risk) ratio (28.4±0.8%) compared with the control group (45.2±1.9%; $P<0.0001$) (Figure 5D). The number of apoptotic cardiomyocytes in infarct border myocardial tissue assessed by TUNEL staining showed that the proportion of apoptotic positive cardiomyocytes in the Ad5:cTNT-SGK3 group (4.1±0.3%) was significantly lower than that in the control group (7.1±0.4%; $P=0.0001$) (Figure 5E).

Next, AAV9 vectors, which take effect 5 to 7 days after injection, were used to investigate the chronic effect of SGK3 overexpression after I/R injury. The AAV9:cTNT-SGK3 (1.1×10^{12} vg/mL, total stock solution=1 µL/mouse, diluted to 9 µL with PBS) or AAV9:cTNT-CON (1.1×10^{12} vg/mL, total stock solution=1 µL/mouse, diluted to 9 µL with PBS) were injected into 3 locations (3 µL for each point) of infarct border myocardium after ischemia operation. The relevant experiments were then performed (details shown in Figure 6A). As expected, Ki67+ cardiomyocytes (CON: 0.4749±0.1287%, SGK3: 1.1197±0.1%; $P=0.0167$) were significantly increased in infarct border zone in AAV9:cTNT-SGK3–treated adult mice, as compared with AAV9:cTNT-CON–treated mice (Figure 6B).

Moreover, the cardiac function index of EF (52.5±1.3%) and FS (27.1±0.8) at 28 days after I/R injury was markedly higher in AAV9:cTNT-SGK3–transfected mice than in AAV9:cTNT-CON–treated mice (EF: 40.4±3.7%, $P=0.009$; FS: 20.0±2.0%, $P=0.0068$) (Figure 6C and 6D). Western blot results at 14 days after I/R injury confirmed the successful transfection of AAV9:cTNT-SGK3 in myocardial tissue (Figure S6B). Scar size (22.3±2.5%, $P=0.0045$) at 28 days after I/R injury was significantly smaller in AAV9:cTNT-SGK3–treated adult mice than that in AAV9:cTNT-CON–treated mice (36.3±3.1%) (Figure 6E and 6F). Similarly, the fibrosis markers reflected by mRNA expression of collagense-1 (CON: 1.767±0.1138%, SGK3: 1.235±0.1118%; $P=0.0075$), collagense-3 (CON: 3.015±0.3256%, SGK3: 1.663±0.2243%; $P=0.0066$), and ACTA2 (actin alpha 2) (CON: 2.98±0.2893%, SGK3: 1.12±0.06426%; $P<0.0001$) was significantly lower in the AAV9:cTNT-SGK3 group than that in the AAV9:cTNT-CON group (Figure 6G through 6I). The overall survival rate up to 28 days after I/R injury was similar between the AAV9:cTNT-SGK3 and AAV9:cTNT-CON groups (Figure 6J).

SGK3 Enhances Cardiomyocyte Regeneration and Heart Function Recovery Through GSK-3β/β-Catenin Pathway After Cardiac Injury

It is known that GSK-3β, β-catenin, mTOR, and cyclin D1 are the key downstream target genes of SGK3.[19–21] Western blot analysis results showed that overexpression of SGK3 activated phosphorylation of GSK-3β at Ser9 and upregulated the expression of β-catenin, but did not affect the expression of phosphorylated-mTOR and mTOR (Figure 7A). 6-bromoindirubin-3'-oxime (BIO: 2 µmol/L), an inhibitor of GSK-3β, was then added into neonatal mouse cardiomyocytes treated with or without Ad5:cTNT-SGK3i in vitro to verify the role of GSK-3β in SGK3-treated cardiomyocytes. EDU
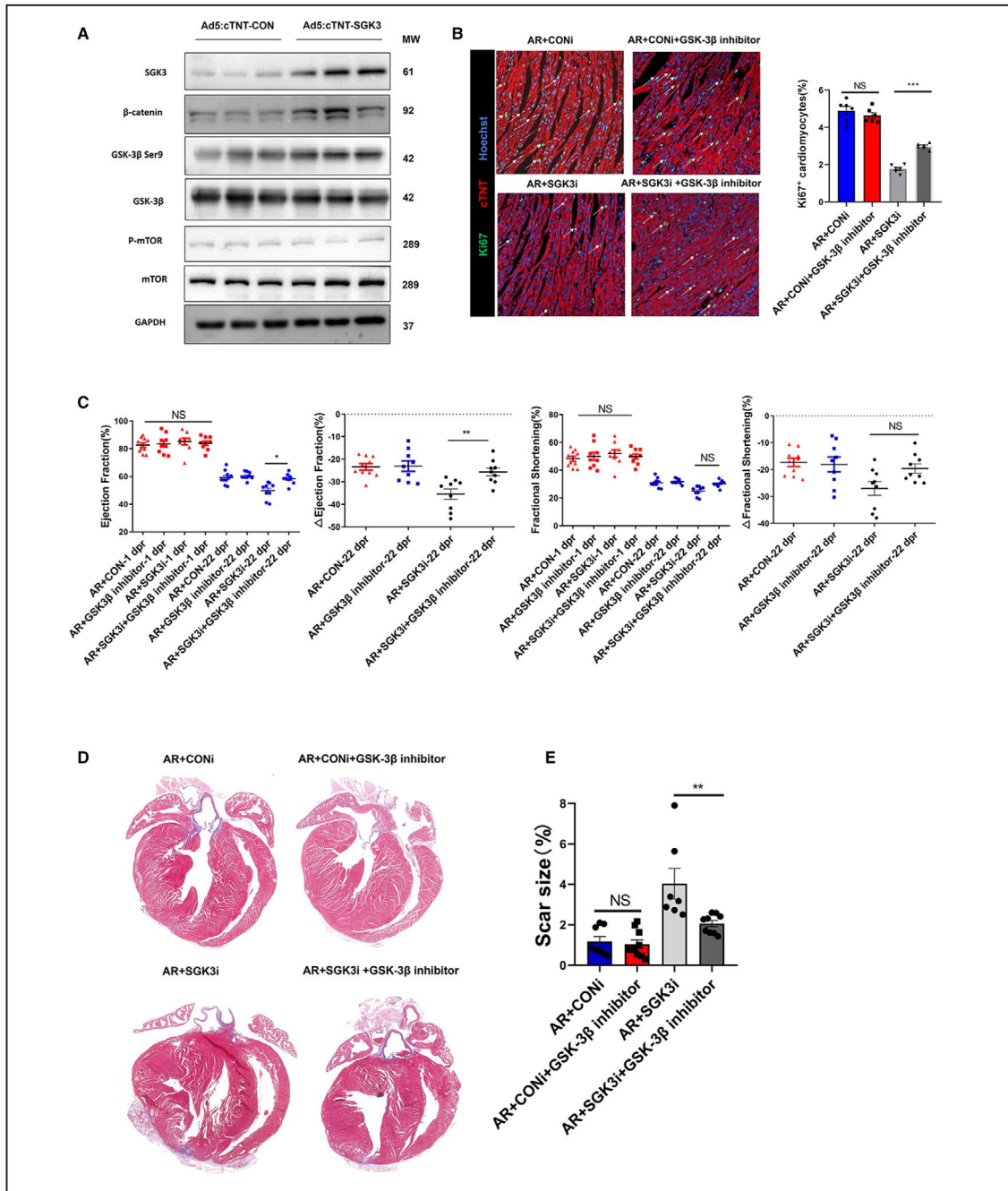
Figure 7. **BIO, an inhibitor of GSK-3β (glycogen synthase kinase-3β), blocks the inhibitory effect of SGK3 (serine/threonine-protein kinase 3) knockdown on cardiac regeneration after apical resection (AR) injury in neonatal mice.**
A, SGK3, GSK-3β, GSK-3β Ser9, β-catenin, p-mTOR, and mTOR protein expression between Ad5:cTNT-CON– and Ad5:cTNT-SGK3–transfected cardiomyocytes. **B**, Immunofluorescence staining of cardiomyocytes in vivo was then performed to detect the cardiomyocyte proliferation for Ki67+ (7717 cardiomyocytes in AR+Ad5:cTNT-CON group, 7771 cardiomyocytes in AR+BIO group, 7456 cardiomyocytes in AR+Ad5:cTNT-SGK3i group and 6915 cardiomyocytes in AR+Ad5:cTNT-SGK3i+BIO group). **C**, Cardiac function of ejection fraction and fractional shortening was evaluated in each group mice (AR+Ad5:cTNT-CON group, n=9; AR+BIO group, n=9; AR+Ad5:cTNT-SGK3i group, n=9; AR+Ad5:cTNT-SGK3i+BIO group, n=9). **D** and **E**, Masson staining of mouse ventricular cross-sections was performed to determine the scar size in each group mice (AR+Ad5:cTNT-CON group, n=8; AR+BIO group, n=9; AR+Ad5:cTNT-SGK3i group, n=7; AR+Ad5:cTNT-SGK3i+BIO group, n=9). Data are presented as mean±SEM. *P≤0.05; **P≤0.01; ***P≤0.001. Ad5:cTNT-CON indicates control adenovirus serotype 5; Ad5:cTNT-SGK3, cardiomyocyte-specific SGK3 overexpression adenovirus serotype 5; Ad5:cTNT-SGK3i, cardiomyocyte-specific SGK3 knockdown adenovirus serotype 5; BIO, 6-bromoindirubin-3'-oxime; CON, control; CONi, knockdown control; dpr, days post resection; GSK-3β Ser9, phosphorylated glycogen synthase kinase-3 beta at Ser9; ki67+, ki67 positivite; mTOR, mechanistic target of rapamycin kinase; NS, no significance; and p-mTOR, phosphorylated-mechanistic target of rapamycin kinase.

staining results showed that GSK-3β inhibition partially blunted the inhibitory role of Ad5:cTNT-SGK3i on cardiomyocyte proliferation (SGK3i: 0.8827±0.07907%, SGK3i+BIO: 1.88±0.1113%; $P<0.0001$) (Figure S7A). To further verify whether the GSK-3β pathway mediates the effect of Ad5:cTNT-SGK3i on cardiomyocyte proliferation and cardiac function recovery after AR in vivo, P1 mice were used to construct the AR+SGK3i model in the absence or presence BIO (5 mg/kg, total volume=9 μL/mouse, intraperitoneally injected once a day for 6 days), the hearts were then collected at 6 days after AR. The number of immunofluorescence-stained Ki67^{+} cardiomyocytes (SGK3i: 1.768±0.09055%, SGK3i+BIO: 2.992±0.06385%; $P<0.0001$), which were decreased by SGK3 inhibition on the resection border zone, was increased after cotreatment with GSK-3β inhibitor (Figure 7B). In addition, at the 22 day after AR, EF (49.7±1.9%) in cardiomyocyte-specific SGK3 knockdown adenovirus treatment mice were markedly increased by cotreatment with BIO (EF: 58.3±1.2%; $P=0.022$) (Figure 7C). Finally, Masson staining results showed that BIO partially reduced fibrous scar in the excised myocardial tissue in Ad:cTNT-SGK3i neonatal mice at postnatal day 22 mice heart (SGK3i: 4.03±0.76%, SGK3i+BIO: 2.05±0.47%; $P=0.0041$) (Figure 7D and 7E).

To further explore the mechanism of SGK3 in regulating cardiomyocyte proliferation, the cardiomyocytes were transfected with Ad5:cTNT-SGK3 or Ad5:cTNT-CON for 48 hours, and mRNA expressions of cell cycle regulatory genes were determined. Quantitative real-time polymerase chain reaction analysis revealed that SGK3 overexpression in cardiomyocytes significantly upregulated the cell cycle promoting genes of cyclin D1, c-myc, and cdc20 (cell division cycle 20) while downregulating the cell cycle inhibiting genes of cardiomyocytes from P21 (cyclin kinase inhibitor P21) and P27 (cyclin kinase inhibitor P27) mice as compared with Ad-CON cardiomyocytes (Figure 8A). Cycline D1 and c-myc are important downstream target genes of β-catenin, and we have shown that SGK3 can upregulate the expression of β-catenin. SGK3 alone or with β-catenin short hairpin RNA were transfected in cardiomyocytes for 48 hours, and the transfection efficiency was evidenced by Western blot analysis (Figure S7B). Immunofluorescence staining showed that the proportion of cardiomyocytes reentering the cell cycle (Ki67^{+}) promoted by Ad5:cTNT-SGK3 was obviously blocked by β-catenin short hairpin RNA ($P<0.0001$) (Figure S7C). In vivo, specific AAV9:cTNT-SGK3 or/and AAV9:cTNT-β-catenin RNA interference intramyocardial injection was made by a microinjector in P56 adult mice underwent I/R injury. At 14 days after reperfusion, Western blot analysis verified the transfection efficiency of AAV9:cTNT-SGK3 and AAV9:cTNT-β-catenin RNAi (Figure 8B). At 28 days after reperfusion,

I/R injury–impaired cardiac function (EF: 43.3±2.8%, FS: 21.5±1.5%) in Ad:cTNT-CON group mice was significantly improved after SGK3 overexpression (EF: 52.5±2.2%, FS: 27.1±1.3%), while β-catenin knockdown resulted in further reduced EF and FS values (EF: 27.6±3.1%, FS: 13.3±1.6%). In addition, EF and FS values in SGK3 overexpression combined with β-catenin knockout group mice were lower (EF: 42.6±3.9%, $P=0.0112$; FS: 21.6±2.3%, $P=0.014$) than in the SGK3 overexpression group (Figure 8C). Meanwhile, SGK3 overexpression-induced reduction in scar size after I/R injury (20.0±2.3%) was blocked in AAV9:cTNT-SGK3 and AAV9:cTNT-β-catenin RNA interference cotransfected hearts (26.0±1.3%, $P=0.0001$) (Figure 8D and 8E). Overall, in view of the significant downregulation of SGK3 expression after P7, we speculate that endogenous SGK3 in cardiomyocytes could hardly affect cardiac repair after ischemic injury in adult hearts. Here, we show that exogenous overexpression of SGK3, especially in cardiomyocytes, could promote myocardial regeneration and inhibit apoptosis, and thus play a protective role in I/R-induced cardiac injury. The role and potential mechanism of SGK3 on neonatal cardiomyocyte regeneration and the therapeutic effect on cardiac repair after I/R injury in adult mice are illustrated in Figure 8F.

DISCUSSION

In the present study, we elaborate that SGK3, which functions as the upstream of the GSK-3β/β-catenin pathway and some kinds of cell cycle regulatory genes, is capable of promoting cardiomyocytes reentering cell cycle through in vitro and in vivo experiments. Along with cardiomyocyte proliferation, SGK3 overexpression robustly attenuated oxygen glucose deprivation/reoxygenation–induced cardiomyocyte apoptosis in vitro and I/R injury–induced cardiomyocyte apoptosis in the infarct border zone in vivo, which is also of great significance for the improvement of and myocardial repair and cardiac function after I/R injury. SGK3 overexpression brings beneficial effects in terms of reducing the ratio of infarction area/area at risk in the acute phase and the long-term fibrous scar size after I/R injury, indicating a strong effect of alleviating postinfarction cardiac remodeling with this strategy. Mechanistically, the beneficial effects are mediated through the GSK-3β/β-catenin pathway. To the best our knowledge, this is the first report describing the effects of SGK3 and related mechanism after cardiac insult.

Based on gain- and loss-of-function study in vitro, we indicated that SGK3 overexpression obviously increased, whereas SGK3 knockdown significantly inhibited the proportion of cardiomyocytes in DNA synthesis and mitotic state. In line with our results, Scortegagna et al also reported that inhibition of SGK3

can significantly reduce the expression of cyclin D1 and the phosphorylation of P70S6K, resulting in the arrest of melanoma cell cycle in the Gap 1 phase.[22] In

contrast, overexpression of SGK3 could increase the phosphorylation level of GSK-3β on Ser9, thus suppressing β-catenin degradation and promoting cell
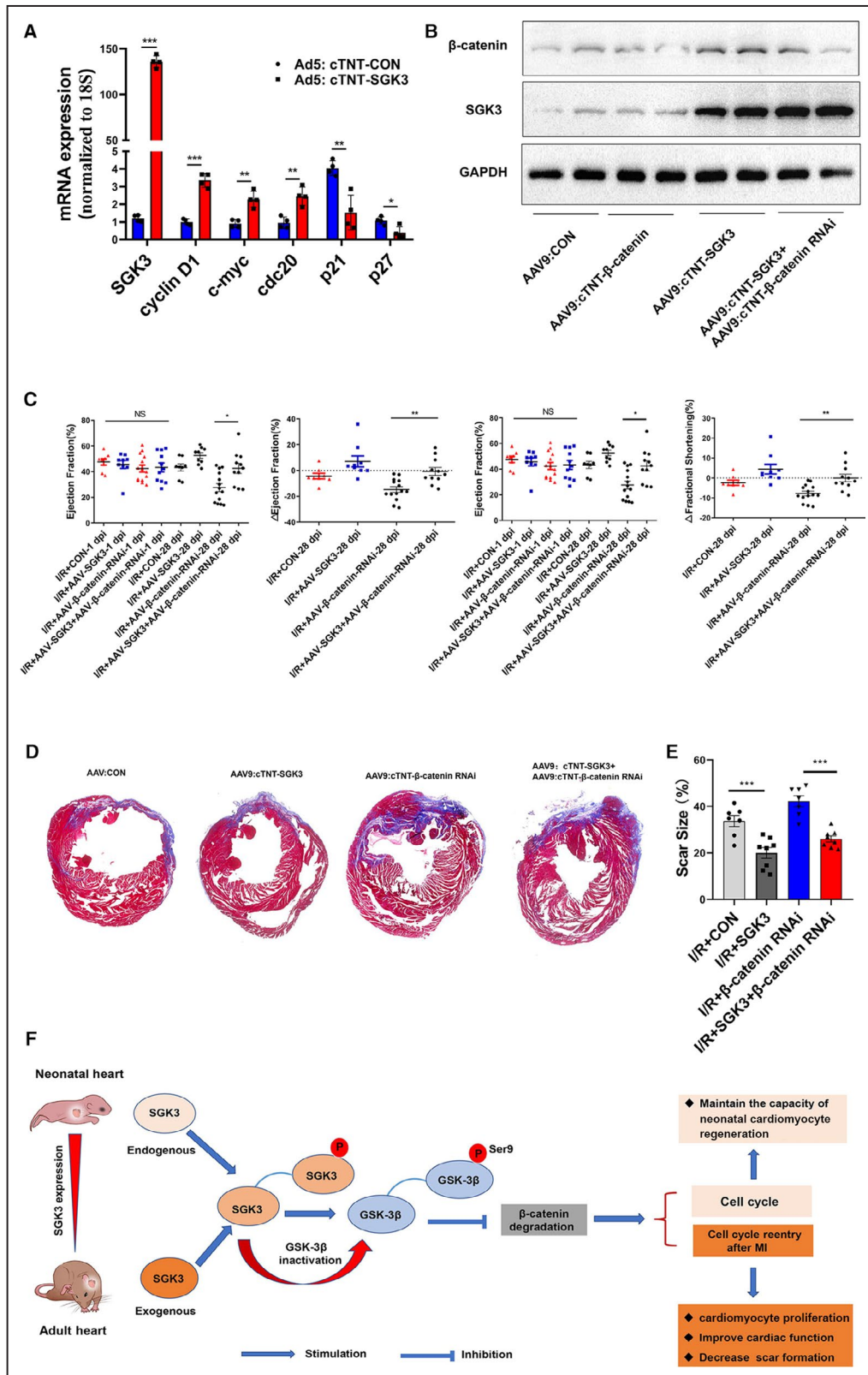
Figure 8. **The cardiac function improvement of SGK3 (serine/threonine-protein kinase 3) on ischemia/reperfusion (I/R)-induced cardiac injury was partially reversed by β-catenin knockdown.**
A, Quantitative real-time polymerase chain reaction analysis was performed to detect the messenger RNA (mRNA) expression of SGK3, cyclin D1, c-myc (cellular-myelocytomatosis viral oncogene), cdc20 (cell division cycle 20), P21 (cyclin kinase inhibitor P21), and P27 (cyclin kinase inhibitor P27). **B**, The AAV9:cTNT-SGK3 was transfected into myocardium with or without AAV9:cTNT-β-catenin RNAi after ischemia, and reperfusion was given after 45 minutes of ischemia. Western blot analysis was then performed to determine the expression of SGK3 and β-catenin after 14 days of I/R. **C**, Cardiac function of ejection fraction and fractional shortening was tested in each group of mice (I/R+AAV9:cTNT-CON group, n=8; I/R+AAV9:cTNT-β-catenin RNAi group, n=14; I/R+AAV9:cTNT-SGK3 group, n=9; I/R+AAV9:cTNT-SGK3+AAV9:cTNT-β-catenin RNAi group, n=12). **D** and **E**, Masson staining of mouse ventricular cross-sections was performed to determine the scar size in each group mice (I/R+AAV9:cTNT-CON group, n=7; I/R+AAV9:cTNT-β-catenin RNAi group, n=7; I/R+AAV9:cTNT-SGK3 group, n=8; I/R+AAV9:cTNT-SGK3i+AAV9:cTNT-β-catenin RNAi group, n=8). **F**, A model illustration of the role and mechanism of SGK3 in promoting cardiomyocyte regeneration and cardiac function recovery in neonatal and adult heart. Transient high expression of SGK3 in the neonatal heart maintains the regeneration ability within 7 days after birth. In the adult heart, the expression and activity of SGK3 is significantly downregulated. Exogenous administration of SGK3 significantly promotes the cardiomyocyte proliferation and cardiac repair after I/R injury. Data are presented as mean±SEM. *$P \leq 0.05$; **$P \leq 0.01$; ***$P \leq 0.001$. 18S indicates 18S ribosomal DNA; AAV, adeno-associated virus serotype; AAV9:cTNT-CON, control adeno-associated virus serotype 9; AAV9:cTNT-SGK3, cardiomyocyte-specific SGK3 overexpression adeno-associated virus serotype 9; CON, control; cyclin D1, G1/S-specific cyclin-D1; dpi, days post infarction; GAPDH, glyceraldehyde-3-phosphate dehydrogenase; GSK-3β, glycogen synthase kinase-3β; MI, myocardial infarction; NS, no significance; P21, postnatal day 21; P27, postnatal day 27; and RNAi, RNA interference.

cycle gene CCND1 expression in hepatocellular carcinoma.[19,23] These results suggest that SGK3 plays an important role in cell cycle regulation. Furthermore, it was also demonstrated that SGK3 overexpression could attenuate oxygen glucose deprivation/reoxygenation and I/R-induced cardiomyocyte apoptosis in vitro and in vivo. The above results indicate that SGK3 can simultaneously exert a dual role in promoting proliferation and inhibiting apoptosis of cardiomyocytes.

Our results are consistent with previous findings, which showed that modulating functional genes could protect against heart injury through promoting proliferation and suppressing apoptosis of cardiomyocytes. For instance, Hauck et al and Magadum et al revealed that Pkm2 (pyruvate kinase muscle isozyme 2) played a crucial role in promoting myocardial proliferation, inhibiting oxidative stress and apoptosis after MI injury.[24,25]

In the neonatal heart, cardiomyocyte-specific SGK3 overexpression adenovirus was used to transfect SGK3 to isolated cardiomyocytes, and the expression of reported downstream proteins of SGK3 related to cardiomyocyte regeneration and cardiac repair was explored.[19,23,26] We found that SGK3 significantly promoted the phosphorylation level of GSK-3β on Ser9 and β-catenin expression, but did not affect the expression of phosphorylated-mTOR and mTOR, suggesting that SGK3 played a role in cardiomyocyte proliferation through mTOR-independent pathways. We also demonstrated that SGK3 can regulate a series of cell cycle genes including β-catenin targets. In cardiomyocytes, GSK-3β is activated by SGK3, which could lead to ubiquitination and degradation of β-catenin in the cytoplasm, and promote the accumulation of β-catenin in the nucleus. Subsequently, as a transcription coactivator of T-cell factor/lymphoid enhancer factor transcription factors, β-catenin could translocate to the nucleus and initiate the transcription

events of target genes.[27,28] These mechanistic data collectively demonstrate that SGK3 might be a critical regulator of cardiomyocyte regeneration and cardiac repair through regulating GSK-3β/β-catenin and cell cycle regulator genes.

The GSK-3β/β-catenin signaling pathway is generally considered as the downstream common pathway to drive the proliferation of cardiomyocytes. For instance, Hippo/Yap, insulin-like growth factor, peroxisome promoter activated receptor delta, and neuregulin/erb-b2 receptor tyrosine kinase 2 signaling pathways have all been reported to be involved in the enhancement of downstream β-catenin signaling to stimulate the cardiomyocyte proliferation.[11,29–31] However, Quaife-Ryan et al recently showed that when the β-catenin signal was directly activated, it could just promote cell proliferation in immature cardiomyocytes, while the activation of the β-catenin signaling pathway can induce cardiomyocyte hypertrophy instead of cardiomyocyte proliferation in mature cardiomyocytes.[32] The possible reason for this phenomenon might be that the transcriptional responses of immature and mature cardiomyocytes to active β-catenin signal differ significantly. β-catenin signal could drive the transcriptional regulatory network of cell cycle–related target genes in immature cardiomyocytes,whereas in mature cardiomyocytes, it is converted to the regulation of the transcriptional program of inflammation, apoptosis, and metabolism-related target genes.[32–34] Although the activation of β-catenin cannot induce mature cardiomyocyte proliferation, it can give rise to cardioprotection response and decrease in scar size after MI in the adult heart.[32] In our study, we observed that the cardiomyocyte-specific overexpression of SGK3 kinase activated downstream β-catenin signal in neonatal and adult cardiomyocytes. The protective effect of SGK3 on the cardiac function recovery and the

fibrous scar size reduction after I/R injury in adult mice was significantly reversed by cardiomyocyte-specific AAV9:cTNT-β-catenin RNA interference, indicating that the β-catenin pathway mediated the protective effect of SGK3 on adult I/R injury.

It is known that AKT and its downstream pathways, including the AKT/GSK-3β pathway, play an important role in cardiac repair after MI injury.[35,36] After cardiac injury, inhibition of GSK-3β activity downstream of AKT improved cardiac function and promoted myocardial repair by enhancing cardiomyocyte proliferation and reducing apoptosis.[37,38] In this study, SGK3 overexpression promoted cardiomyocyte proliferation and ameliorated adult I/R injury, and increased phosphorylation level of GSK-3β at ser9, which is linked to GSK-3β activity inhibition. In line with these results, inhibition of GSK-3β activity significantly blocked the inhibitory effect of SGK3 knockdown on cardiomyocyte proliferation and cardiac function recovery after AR in neonatal mice. Although SGK3 is highly homologous with AKT in structure, and multiple substrates of SGK3 are also regulated by AKT, including GSK-3β/β-catenin signaling,[23] some downstream AKT signaling is not mediated by AKT in some types of cells, but is dependent on other signaling, such as SGK3.[39,40] Previously, Liu et al also reported the role of SGK3 in the progression of hepatocellular carcinoma via AKT independent pathways.[23] In view of the complexity of the PI3K pathway, future studies are warranted to explore if other downstream signaling of SGK3 pathways also mediated the effects of exogenous introduction of SGK3 and promoted cardiomyocyte regeneration and cardiac repair in adult mice post MI, in addition to the defined GSK-3β/β-catenin pathway.

Although our current results provide convincing evidence to support the effects of SGK3 in cardiac repair after I/R, several issues should be considered in interpretation of present results. One of the concerns is the specificity of SGK3 action. As a potential carcinogenic kinase, it is necessary to achieve transient-specific overexpression in myocardial tissue after MI, so as to improve cardiac repair and reduce adverse effects on other organ systems. Another limitation of this study is that no commercial isoform-specific SGK3 inhibitors are available currently, which hindered further investigating on the molecular mechanism of SGK3 in promoting cardiomyocyte proliferation.

In conclusion, we explored the potential cardioprotective effect of SGK3 kinase, and proved the cardiac protective role of SGK3 through GSK3β and β-catenin. The present findings extend our knowledge on the kinase regulatory network of myocardial regeneration and indicate that targeting the SGK3 and GSK3β/β-catenin pathway might have therapeutic implication on cardiac repair after heart injury.

REFERENCES

1. Bai LI, Shin S, Burnett RT, Kwong JC, Hystad P, van Donkelaar A, Goldberg MS, Lavigne E, Copes R, Martin RV, et al. Exposure to ambient air pollution and the incidence of congestive heart failure and acute myocardial infarction: a population-based study of 5.1 million Canadian adults living in Ontario. *Environ Int*. 2019;132:105004. doi: 10.1016/j.envint.2019.105004

2. Du C, Fan Y, Li YF, Wei TW, Wang LS. Research progress on myocardial regeneration: what is new? *Chin Med J (Engl)*. 2020;133:716–723. doi: 10.1097/CM9.0000000000000693

3. Deshmukh V, Wang J, Martin JF. Leading progress in heart regeneration and repair. *Curr Opin Cell Biol*. 2019;61:79–85. doi: 10.1016/j.ceb.2019.07.005

4. Chien KR, Frisen J, Fritsche-Danielson R, Melton DA, Murry CE, Weissman IL. Regenerating the field of cardiovascular cell therapy. *Nat Biotechnol*. 2019;37:232–237. doi: 10.1038/s41587-019-0042-1

5. Gao F, Kataoka M, Liu N, Liang T, Huang Z-P, Gu F, Ding J, Liu J, Zhang F, Ma Q, et al. Therapeutic role of miR-19a/19b in cardiac regeneration and protection from myocardial infarction. *Nat Commun*. 2019;10:1802. doi: 10.1038/s41467-019-09530-1

6. Fan YI, Cheng Y, Li Y, Chen B, Wang Z, Wei T, Zhang H, Guo Y, Wang Q, Wei Y, et al. Phosphoproteomic analysis of neonatal regenerative myocardium revealed important roles of checkpoint kinase 1 via activating

mammalian target of rapamycin C1/ribosomal protein S6 kinase b-1 pathway. *Circulation*. 2020;141:1554–1569. doi: 10.1161/CIRCULATIO NAHA.119.040747

7. Borden A, Kurian J, Nickoloff E, Yang Y, Troupes CD, Ibetti J, Lucchese AM, Gao E, Mohsin S, Koch WJ, et al. Transient introduction of miR-294 in the heart promotes cardiomyocyte cell cycle reentry after injury. *Circ Res*. 2019;125:14–25. doi: 10.1161/CIRCRESAHA.118.314223

8. Mohamed TMA, Ang YS, Radzinsky E, Zhou P, Huang Y, Elfenbein A, Foley A, Magnitsky S, Srivastava D. Regulation of cell cycle to stimulate adult cardiomyocyte proliferation and cardiac regeneration. *Cell*. 2018;173:104–116.e12. doi: 10.1016/j.cell.2018.02.014

9. Wang J, Liu S, Heallen T, Martin JF. The Hippo pathway in the heart: pivotal roles in development, disease, and regeneration. *Nat Rev Cardiol*. 2018;15:672–684. doi: 10.1038/s41569-018-0063-3

10. Ponnusamy M, Li PF, Wang K. Understanding cardiomyocyte proliferation: an insight into cell cycle activity. *Cell Mol Life Sci*. 2017;74:1019–1034. doi: 10.1007/s00018-016-2375-y

11. D'Uva G, Aharonov A, Lauriola M, Kain D, Yahalom-Ronen Y, Carvalho S, Weisinger K, Bassat E, Rajchman D, Yifa O, et al. ERBB2 triggers mammalian heart regeneration by promoting cardiomyocyte dedifferentiation and proliferation. *Nat Cell Biol*. 2015;17:627–638.

12. Lang F, Bohmer C, Palmada M, Seebohm G, Strutz-Seebohm N, Vallon V. (Patho)physiological significance of the serum- and glucocorticoid-inducible kinase isoforms. *Physiol Rev*. 2006;86:1151–1178. doi: 10.1152/physrev.00050.2005

13. Basnet R, Gong GQ, Li C, Wang MW. Serum and glucocorticoid inducible protein kinases (SGKs): a potential target for cancer intervention. *Acta Pharm Sin B*. 2018;8:767–771. doi: 10.1016/j.apsb.2018.07.001

14. Beigi F, Schmeckpeper J, Pow-Anpongkul P, Payne JA, Zhang L, Zhang Z, Huang J, Mirotsou M, Dzau VJ. C3orf58, a novel paracrine protein, stimulates cardiomyocyte cell-cycle progression through the PI3K-AKT-CDK7 pathway. *Circ Res*. 2013;113:372–380.

15. Wang H, Huang F, Zhang Z, Wang P, Luo Y, Li H, Li NA, Wang J, Zhou J, Wang Y, et al. Feedback activation of SGK3 and AKT contributes to rapamycin resistance by reactivating mTORC1/4EBP1 axis via TSC2 in breast cancer. *Int J Biol Sci*. 2019;15:929–941. doi: 10.7150/ijbs.32489

16. Bhandaru M, Kempe DS, Rotte A, Capuano P, Pathare G, Sopjani M, Alesutan I, Tyan L, Huang DY, Siraskar B, et al. Decreased bone density and increased phosphaturia in gene-targeted mice lacking functional serum- and glucocorticoid-inducible kinase 3. *Kidney Int*. 2011;80:61–67. doi: 10.1038/ki.2011.67

17. Peng LQ, Zhao H, Liu S, Yuan YP, Yuan CY, Mwamunyi MJ, Pearce D, Yao LJ. Lack of serum- and glucocorticoid-inducible kinase 3 leads to podocyte dysfunction. *FASEB J*. 2018;32:576–587. doi: 10.1096/fj.201700393RR

18. McCormick JA, Feng Y, Dawson K, Behne MJ, Yu B, Wang J, Wyatt AW, Henke G, Grahammer F, Mauro TM, et al. Targeted disruption of the protein kinase SGK3/CISK impairs postnatal hair follicle development. *Mol Biol Cell*. 2004;15:4278–4288. doi: 10.1091/mbc.e04-01-0027

19. Liu F, Wu X, Jiang X, Qian Y, Gao J. Prolonged inhibition of class I PI3K promotes liver cancer stem cell expansion by augmenting SGK3/GSK-3beta/beta-catenin signalling. *J Exp Clin Cancer Res*. 2018;37:122.

20. Wang Y, Zhou D, Chen S. SGK3 is an androgen-inducible kinase promoting prostate cancer cell proliferation through activation of p70 S6 kinase and up-regulation of cyclin D1. *Mol Endocrinol*. 2014;28:935–948. doi: 10.1210/me.2013-1339

21. Bago R, Sommer E, Castel P, Crafter C, Bailey FP, Shpiro N, Baselga J, Cross D, Eyers PA, Alessi DR. The hVps34-SGK3 pathway alleviates sustained PI3K/Akt inhibition by stimulating mTORC1 and tumour growth. *EMBO J*. 2016;35:2263.

22. Scortegagna M, Lau E, Zhang T, Feng Y, Sereduk C, Yin H, De SK, Meeth K, Platt JT, Langdon CG, et al. PDK1 and SGK3 contribute to the growth of BRAF-mutant melanomas and are potential therapeutic targets. *Cancer Res*. 2015;75:1399–1412. doi: 10.1158/0008-5472.CAN-14-2785

23. Liu M, Chen L, Chan TH, Wang J, Li Y, Li Y, Zeng TT, Yuan YF, Guan XY. Serum and glucocorticoid kinase 3 at 8q13.1 promotes cell proliferation and survival in hepatocellular carcinoma. *Hepatology*. 2012;55:1754–1765. doi: 10.1002/hep.25584

24. Magadum A, Singh N, Kurian AA, Munir I, Mehmood T, Brown K, Sharkar MTK, Chepurko E, Sassi Y, Oh JG, et al. Pkm2 regulates cardiomyocyte cell cycle and promotes cardiac regeneration. *Circulation*. 2020;141:1249–1265. doi: 10.1161/CIRCULATIONAHA.119.043067

25. Hauck L, Dadson K, Chauhan S, Grothe D, Billia F. Inhibiting the Pkm2/b-catenin axis drives in vivo replication of adult cardiomyocytes following experimental MI. *Cell Death Differ*. 2021;28:1398–1417. doi: 10.1038/s41418-020-00669-9

26. Bago R, Sommer E, Castel P, Crafter C, Bailey FP, Shpiro N, Baselga J, Cross D, Eyers PA, Alessi DR. The hVps34-SGK3 pathway alleviates sustained PI3K/Akt inhibition by stimulating mTORC1 and tumour growth. *EMBO J*. 2016;35:1902–1922.

27. Huang S, Li X, Zheng H, Si X, Li B, Wei G, Li C, Chen Y, Chen Y, Liao W, et al. Loss of super-enhancer-regulated circRNA Nfix induces cardiac regeneration after myocardial infarction in adult mice. *Circulation*. 2019;139:2857–2876. doi: 10.1161/CIRCULATIONAHA.118.038361

28. Lin J, Song T, Li C, Mao W. GSK-3beta in DNA repair, apoptosis, and resistance of chemotherapy, radiotherapy of cancer. *Biochim Biophys Acta*. 2020;1867:118659.

29. Yu FX, Zhao B, Guan KL. Hippo pathway in organ size control, tissue homeostasis, and cancer. *Cell*. 2015;163:811–828. doi: 10.1016/j.cell.2015.10.044

30. Magadum A, Ding Y, He L, Kim T, Vasudevarao MD, Long Q, Yang K, Wickramasinghe N, Renikunta HV, Dubois N, et al. Live cell screening platform identifies PPARdelta as a regulator of cardiomyocyte proliferation and cardiac repair. *Cell Res*. 2017;27:1002–1019.

31. Xin M, Kim Y, Sutherland LB, Qi X, McAnally J, Schwartz RJ, Richardson JA, Bassel-Duby R, Olson EN. Regulation of insulin-like growth factor signaling by Yap governs cardiomyocyte proliferation and embryonic heart size. *Sci Signal*. 2011;4:ra70. doi: 10.1126/scisignal.2002278

32. Quaife-Ryan GA, Mills RJ, Lavers G, Voges HK, Vivien CJ, Elliott DA, Ramialison M, Hudson JE, Porrello ER. Beta-catenin drives distinct transcriptional networks in proliferative and nonproliferative cardiomyocytes. *Development*. 2020;147:dev193417.

33. Mills RJ, Titmarsh DM, Koenig X, Parker BL, Ryall JG, Quaife-Ryan GA, Voges HK, Hodson MP, Ferguson C, Drowley L, et al. Functional screening in human cardiac organoids reveals a metabolic mechanism for cardiomyocyte cell cycle arrest. *Proc Natl Acad Sci USA*. 2017;114:E8372–E8381. doi: 10.1073/pnas.1707316114

34. Wang W, Hu C-K, Zeng AN, Alegre D, Hu D, Gotting K, Ortega Granillo A, Wang Y, Robb S, Schnittker R, et al. Changes in regeneration-responsive enhancers shape regenerative capacities in vertebrates. *Science*. 2020;369:eaaz3090. doi: 10.1126/science.aaz3090

35. Hernandez-Resendiz S, Palma-Flores C, De Los SS, Roman-Anguiano NG, Flores M, de la Pena A, Flores PL, Fernandez GJ, Coral-Vazquez RM, Zazueta C. Reduction of no-reflow and reperfusion injury with the synthetic 17beta-aminoestrogen compound Prolame is associated with PI3K/Akt/eNOS signaling cascade. *Basic Res Cardiol*. 2015;110:1.

36. Smith CC, Yellon DM. Adipocytokines, cardiovascular pathophysiology and myocardial protection. *Pharmacol Ther*. 2011;129:206–219. doi: 10.1016/j.pharmthera.2010.09.003

37. Kerkela R, Kockeritz L, Macaulay K, Zhou J, Doble BW, Beahm C, Greytak S, Woulfe K, Trivedi CM, Woodgett JR, et al. Deletion of GSK-3beta in mice leads to hypertrophic cardiomyopathy secondary to cardiomyoblast hyperproliferation. *J Clin Invest*. 2008;118:3609–3618.

38. Benard L, Oh JG, Cacheux M, Lee A, Nonnenmacher M, Matasic DS, Kohlbrenner E, Kho C, Pavoine C, Hajjar RJ, et al. Cardiac Stim1 silencing impairs adaptive hypertrophy and promotes heart failure through inactivation of mTORC2/Akt signaling. *Circulation*. 2016;133:1458–1471; discussion 1471.

39. Vasudevan KM, Barbie DA, Davies MA, Rabinovsky R, McNear CJ, Kim JJ, Hennessy BT, Tseng H, Pochanard P, Kim SY, et al. AKT-independent signaling downstream of oncogenic PIK3CA mutations in human cancer. *Cancer Cell*. 2009;16:21–32. doi: 10.1016/j.ccr.2009.04.012

40. Bruhn MA, Pearson RB, Hannan RD, Sheppard KE. Second AKT: the rise of SGK in cancer signalling. *Growth Factors*. 2010;28:394–408. doi: 10.3109/08977194.2010.518516

41. Lindsey ML, Bolli R, Canty JM Jr, Du X-J, Frangogiannis NG, Frantz S, Gourdie RG, Holmes JW, Jones SP, Kloner RA, et al. Guidelines for experimental models of myocardial ischemia and infarction. *Am J Physiol Heart Circ Physiol*. 2018;314:H812–H838. doi: 10.1152/ajpheart.00335.2017

42. Xiao J, Liu H, Cretoiu D, Toader DO, Suciu N, Shi J, Shen S, Bei Y, Sluijter JPG, Das S, et al. miR-31a-5p promotes postnatal cardiomyocyte proliferation by targeting RhoBTB1. *Exp Mol Med*. 2017;49:e386. doi: 10.1038/emm.2017.150

Supplemental Material

Data S1.

Supplemental Methods

Animal model construction and intervention

Apical resection (AR) on neonatal (P1) mice (n=139, and 117 survived the operation.) was carried out as previously described.[6] Briefly, P1 mice were anesthetized by cooling on an ice bed for 3 min. Lateral thoracotomy at the fourth intercostal space was performed by blunt dissection of the intercostal muscles following skin incision. Approximately one square millimeter of the apical myocardium was removed perpendicular to the long axis of the heart. After AR, the thoracic wall and skin incision was sutured with 6.0 non-absorbable silk sutures. All P1 mice were then placed under a heat lamp until recovery and returned to their mother.

The injection of adenovirus (AR+ Ad5: cTNT-SGK3i, n=71; AR+ Ad5: cTNT-CONi, n=68) was performed right after the removal of apex myocardium, 62 survived mice in SGK3i group and 55 survived mice in CONi group were investigated in subsequent experiments. The stock solution of adenovirus was diluted with 10% trypan blue solution in PBS (The total amount of virus injected was $1.5*10^7$PFU). A microsyringe with a 36G needle was used for adenovirus injection around the apex of the P1 heart. Needle was inserted into the left ventricle from apex, and injection was made on three locations around the apex (front, middle and back: 2μl for each point) respectively from the endocardium.

The EDU solution was diluted by PBS to a concentration of 5 μg/ul and was injected intraperitoneally at 350 μg at the 4th day post AR (4 dpr). Cardiac function was assessed by echocardiography at 1dpr and 22 dpr (n=10 mice each group). The infarct area was assessed by Masson staining

Myocardial ischemia-reperfusion injury (I/R) was performed in P56 mice (n=159, and 125 survived the operation) as previously described.[41] Briefly, P56 mice were intraperitoneally anesthetized with 1.2% Avertin (Sigma-Aldrich, St. Louis, USA) and artificially ventilated following tracheal intubation. Lateral thoracotomy at the fourth intercostal space was performed by blunt dissection of the intercostal muscles following skin incision. The PE10 catheter was placed on the surface of the heart parallel to the LAD. The LAD and the catheter were then ligated with 7.0 non-absorbable silk sutures for 45 min. The coronary artery occlusion was confirmed by ST-segment elevation in electrocardiography and myocardial color change. After that, the reperfusion was achieved by the withdrawal of the catheter. Following the reperfusion, the thoracic wall and skin incision was sutured with 3.0 non-absorbable silk sutures. All I/R mice were then placed on the heat stage until recovery.

The injection of adeno-associated virus injection (I/R+AAV9: cTNT-SGK3, n=76, I/R+AAV9:cTNT-CON, n=83) was performed in P56 mice following the ligation of LAD and 125 mice survived. A microsyringe with a 36G needle was used for adenovirus injection around the apex of the P56 heart (The total amount of virus injected was $1.5*10^9$v.g.). The needle was inserted into the left ventricle from apex, and injection was made on three locations around the apex (the front, middle and back: 3μl

for each point) respectively from the endocardium. Cardiac function was assessed by echocardiography at 1dpi and 28dpi (n=10 mice each group). The infarct area was assessed by Masson staining.

The adeno-associated virus (I/R+ Ad5:cTNT-SGK3, n=25, I/R+Ad5:cTNT-CON, n=27) was injected in P56 mice following the ligation of LAD, of which 41 mice survived. The injection procedure is same as I/R+AAV9 groups listed above (The total amount of Ad5 injected was $7.5*10^7$PFU). Cardiac function was assessed by echocardiography at 1 hour and 2 days post I/R operation. TTC and TUNEL staining were performed 2 days post operation.

Quantification of infarct size

Mice were re-anesthetized and re-intubated 2 days after reperfusion. The LAD coronary artery was re-occluded by ligating the suture in the same position. Animals were executed and then 1 ml of 1% Evans Blue dye was infused i.v. to define the area at risk (AAR, representing the myocardium lacking blood flow, i.e. negative for blue dye staining). After OCT embedding, transversal sections (n=8, 1-2mm) were cut from the apex to the ventricle. Slices were incubated in triphenyltetrazolium chloride (1% TTC, Sigma) at 37℃ for 30 min to identify the infarcted myocardium. The sections were emerged in formaldehyde overnight. A camera was used to take pictures of four sections of heart tissue in sequence. Regions negative for Evans Blue staining (AAR) and TTC (infarcted myocardium) were then re-photographed and quantified with ImageJ software. % of AAR was determined as the percentage of the area of AAR to LV, and % of infarct size was determined as the percentage of the area of infarcted

myocardium to AAR averaged from the four sections.

At 28 dpi post-reperfusion, mice were sacrificed under deep anesthesia (n=7), then hearts were harvested and fixed overnight in 4% paraformaldehyde, and then embedded in paraffin. Transverse serial sections (5 μm) were obtained from apex to ventricle at an interval of more than 150 μm, then dewaxed by gradient alcohol and rehydrated for Masson staining under standard procedures and infarct area (blue regions) versus the total left ventricular area was quantified using Image J software.

Cardiomyocyte isolation, culture and intervention

Neonatal mice CMs were isolated from 1-3-day-old ICR mice (50-150 mice each time) as previously described.[42] Briefly, after 75% alcohol epidermis disinfection, neonatal mice ventricular myocardium were collected. The ventricular muscle was then shredded and washed out most of red blood cells. Heart tissues were digested with 20 ml digestive solution containing 0.06 g/100ml trypsin (Sigma, USA) and 0.04 g/100ml collagenase II (Worthington, USA) for 6-7 minutes each time until the myocardia tissues were digested into single cells. After incubation with DMEM containing 10% FBS for 45 min, the adherent fibroblasts were removed. The collected suspension was then centrifuged with Percoll liquid (3000 rpm, 30 minutes, slowly rising and falling) to separate CMs from fibroblasts. After discarding the fibroblasts in the upper layer, the CMs in the middle layer were collected and cultured in incubator with 5% CO_2 at 37 ℃. After 24 hours of culture, the cells without adherence were washed out, and the cells were incubated for another 24 hours and then transfected with plasmids or adenoviruses for different experiments.

To explore the functional role of SGK3 on CMs, CMs were transfected with Ad5: cTNT-SGK3 or Ad5: cTNT-SGK3i for 48 h.

Oxygen glucose deprivation/ reoxygenation (OGD/R)

After being washed three times with phosphate buffered saline (PBS), primary neonatal CMs were incubated with glucose and serum free DMEM in AnaeroPACK Rectangular Jar (Mitsubishi gas chemical company, INC, Japan) with 95% N_2 and 5% CO_2 at 37℃. After 8 hours the medium was replaced with DMEM containing 10% FBS and 1% PS. CMs were then placed in an incubator with 5% CO2 balanced with air at 37℃ for 12 hours.

Recombinant adenovirus and plasmid

Recombinant Adenovirus of SGK3 (Ad5:cTNT-SGK3) and Adenovirus of control (Ad5:cTNT-CON) were designed by CM specific cTNT promoter obtained from Genechem Company (Shanghai, China). Adenoviruses carrying scrambled shRNA for mouse SGK3 (Ad5: cTNT-SGK3i) and adenovirus of control (Ad5: cTNT-CONi) were also purchased from Genechem Company (Shanghai, China).

The Adeno associated virus type 9 (AAV9) driven by CM specific cTNT promoter cTNT:3Flag-SGK3 (AAV9:cTNT-SGK3) and control Adeno associated virus type 9 (AAV9:cTNT-CON) were purchased from company Hanbio Company (Hanbio, Shanghai, China). The Adeno associated virus type 9 (AAV9) carrying scrambled shRNA for mouse β-catenin (AAV9: cTNT-β-catenin RNAi) and Adeno associated virus type 9 (AAV9:cTNT-CONi) were also purchased from Genechem Company (Shanghai, China).

Preparation of nuclear and cytoplasmic extracts

The myocardial tissue was grinded and lysed with cytoplasmic lysate (including 0.1% phenylmethylsulfonyl fluoride, 0.1% protease inhibitor, 1% phosphatase inhibitor, 1% cocktail) and then placed on ice for 1 hour. After centrifugation (4 °C, 14000rpm, 20min), the supernatant is cytoplasmic protein. Then, the precipitate was washed three times with precooled PBS, and then added with nuclear cracking solution. After blowing and mixing, the precipitate was ultrasonic (energy 25%, 4 °C, 3 seconds) for three times, and then the cracking solution was placed on ice for about 1 hour. The supernatant obtained after centrifugation is nucleoprotein. Cytoplasmic and nuclear fractionations were homogenized according to nuclear and cytoplasmic extraction reagent kit (Thermo Fisher, USA).

Histological and immunohistochemical staining

To determine the effects of SGK3 on the infarct size, we collected the hearts after MI with SGK3 specifically overexpression in myocardial tissue. The collected hearts were embedded in paraffin, and 5 μm thick cross section was prepared. Each heart was cut into 5 transversal sections (5μm) at 150-200μm interval from apex to base, and each section was stained by Masson staining according to the standard procedure. Finally, the infarct area and total left ventricular area were quantified by Image J software.

Measurement of cardiac function by echocardiography

AR and adenovirus injection (AR+Ad5: cTNT-SGK3i) or AR and adenovirus carrying vector injection (AR+Ad5:cTNT-CONi) was performed in P1 mice. Echocardiography was used to evaluate cardiac function at 1 and 22 dpr

(AR+Ad5:cTNT-CONi group; AR+ Ad5: cTNT-SGK3i group).

I/R and adeno-associated virus injection (I/R+Ad5: cTNT-SGK3) or I/R and adeno-associated virus carrying vector injection (I/R+Ad5: cTNT-CON) were performed in P56 mice. Cardiac function was assessed by echocardiography at 1 hour and 2 dpi (I/R+ Ad5: CON group; I/R+ Ad5: cTNT-SGK3 group).

I/R and adeno-associated virus injection (I/R+AAV9:cTNT-SGK3) or I/R and adeno-associated virus carrying vector injection (I/R+AAV9:cTNT-CON) were performed in P56 mice. Cardiac function was assessed by echocardiography at 1 and 28 dpi (I/R+ AAV9: cTNT-CON group; I/R+ AAV9: cTNT-SGK3 group).

Table S1. The sequences of RT-PCR primers.

Primer(mouse)	Sequence (5'to3')
18S-F	TAACGAACGAGACTCTGGCAT
18S-R	CGGACATCTAAGGGCATCACAG
MAST3-F	CTCTGTCCCAACTGCAGGTAA
MAST3-R	AGTGACCATCTTCTGCCGTC
MASTL-F	TCGGCAAGTGAGGAGAATGAA
MASTL-R	TTTGACAACCTTCACTGCGTACA
NDR1-F	CTCATCGGCTACCCACCATT
NDR1-R	ATCAGGCCCTTGGCTTTCTC
NDR2-F	GACACCGGCAGTTCCAGTTA
NDR2-R	TTCTCCAGTGTGAGCTTGGC
RSKL1-F	TGCTTAGTGCTGCGTGGAG
RSKL1-R	TGAAACAACCCGTGCGGTAA
YANK2-F	GAGAGAAACTCAGGAGGCAGC
YANK2-R	CAGACAGTGTCATCTGGGCA
STLK3-F	TACGAGCTCCAGGAGGTTATC
STLK3-R	ATGGCTTGAATTTCTTTCAGGAG
MAST4-F	TGCTGTGCACTCAGTAGGAG
MAST4-R	GTATTGGCGTTGGAGCTTGG
SGK3-F	TTCTCTTATGCACCTCCTTCA
SGK3-R	ATGGCAAACTGCTCACAAA

STAT1-F	TGCTCCCTCTCTGGAATG
STAT1-R	CTCCTTGCTGATAAGCC
TLR3-F	GGGATTGGTGAGTCTGAAGT
TLR3-R	AGTGAGCAAGGGAGAATGAG
IRF7-F	CCCATCTTCGACTTCAGCA
IRF7-R	TGCCCAAAACCCAGGTAG
cyclin D1-F	GCGTACCCTGACACCAATCTC
cyclin D1-R	ACTTGAAGTAAGATACGGAGGGC
c-myc-F	AGGCAGCTCTGGAGTGAGAG
c-myc-R	CCTGGCTCGCAGATTGTAAG
cdc20-F	TTCGTGTTCGAGAGCGATTTG
cdc20-R	ACCTTGGAACTAGATTTGCCAG
P21-F	CCTGGTGATGTCCGACCTG
P21-R	CCATGAGCGCATCGCAATC
P27-F	TCAAACGTGAGAGTGTCTAACG
P27-R	CCGGGCCGAAGAGATTTCTG
Colla1-F	CAGAGGCGAAGGCAACA
Colla1-R	GTCCAAGGGAGCCACATC
Colla3-F	AGAACCTGGCCGAGATG
Colla3-R	TGGACTTCCGGGCATAC
ACTA2-F	GCCCAGAGCAAGAGAGG
ACTA2-R	TGTCAGCAGTGTCGGATG

Table S2. Statistic data source (see Excel file).

Table S3. Fisher's exact test for enrichment analysis of each predicted kinase in

the KSN by iGPS.

Kinase.ID	Kinase.Name	a(tar sig)	b(tol sig-tar sig)	c(tar all)	d(tol all-tar all)	ER	p	p.adj
Q91YS8	CaMK1a	6	536	36	16189	5.0333	0.002164	0.0547
Q9D7B0	MAP2K2	11	531	113	16112	2.9534	0.002287	0.0547
Q1HKZ5	LZK	10	532	101	16124	3.0005	0.003185	0.0619
B2RTJ7	HH498	10	532	101	16124	3.0005	0.003185	0.0619
O55222	ILK	10	532	101	16124	3.0005	0.003185	0.0619
Q9WVS7	MAP2K5	10	532	102	16123	2.9709	0.003399	0.0622
Q8CE90	MAP2K7	10	532	103	16122	2.9418	0.003624	0.0626
Q9ERE3	**SGK3**	**9**	**533**	**87**	**16138**	**3.1318**	**0.003864**	**0.0632**
Q99MK8	BARK1	11	531	125	16100	2.6679	0.004665	0.0725
Q91VJ4	NDR1	8	534	77	16148	3.1414	0.006158	0.0725
Q3TBR3	PKN2	8	534	77	16148	3.1414	0.006158	0.0725
Q7TSJ6	LATS2	6	536	47	16178	3.8528	0.00703	0.0725
Q9JJX8	YANK2	8	534	81	16144	2.9855	0.008085	0.0725
Q8QZV4	YANK3	8	534	81	16144	2.9855	0.008085	0.0725
Q811L6	MAST4	8	534	81	16144	2.9855	0.008085	0.0725
Q3U214	MAST3	8	534	81	16144	2.9855	0.008085	0.0725
Q8BLK9	RSKL1	8	534	81	16144	2.9855	0.008085	0.0725
A2AQY2	MASTL	8	534	81	16144	2.9855	0.008085	0.0725
Q8BYR2	LATS1	8	534	81	16144	2.9855	0.008085	0.0725

Q8R2S1	RSKL2	8	534	81	16144	2.9855	0.008085	0.0725
Q5SYL1	SgK494	8	534	81	16144	2.9855	0.008085	0.0725
Q80TN1	CaMK2a	14	528	192	16033	2.2140	0.008327	0.0725
P70268	PKN1	6	536	49	16176	3.6945	0.008411	0.0725
B1AST8	MAST2	6	536	49	16176	3.6945	0.008411	0.0725
Q9ESL4	ZAK	7	535	65	16160	3.2525	0.008528	0.0725
B1ASQ8	AMPKa2	8	534	82	16143	2.9490	0.00863	0.0725
B2KFR4	NDR2	8	534	83	16142	2.9133	0.009202	0.0734
Q9R1L5	MAST1	8	534	83	16142	2.9133	0.009202	0.0734
Q923T9	CaMK2g	14	528	196	16029	2.1683	0.00946	0.0735
Q9QYK9	CaMK1b	6	536	52	16173	3.4811	0.010832	0.0780
Q8BGR3	CaMK4	6	536	52	16173	3.4811	0.010832	0.0780
Q8BW96	CAMK1d	6	536	52	16173	3.4811	0.010832	0.0780
Q6GSA6	AKT1	32	510	597	15628	1.6424	0.011034	0.0780
Q9WUA6	AKT3	32	510	601	15624	1.6311	0.011503	0.0794
Q5SVJ0	CaMK2b	6	536	53	16172	3.4152	0.011739	0.0794

Note: a. The number of significantly up-regulated phosphorylation sites annotated with the kinase; b. The number of significantly up-regulated phosphorylation sites annotated without the kinase; c. The number of identified phosphorylation sites annotated with the kinase from this phosphoproteome study; d. The number of identified phosphorylation sites annotated without the kinase from this phosphoproteome study. ER: Enrichment ratio. P: P-value of Fisher's exact test. FDR-q: Adjusted P-value of Fisher's exact test. Benjamini-Hochberg (BH) method was used for multiple testing correction in adjusted P-value calculation.

Figure S1. Decreased cardiac proliferation after birth in mice.
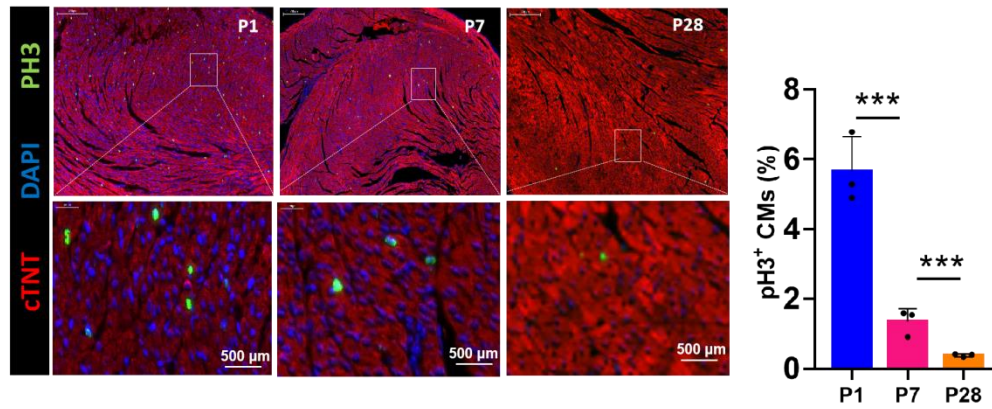
pH3 positive cells representing CM proliferation were detected by immunofluorescence staining at P1 (5140 CMs in P1 group, n=3), P7 (8766 CMs in P7 group, n=3) and P28 (4660 CMs in P28 group, n=3).
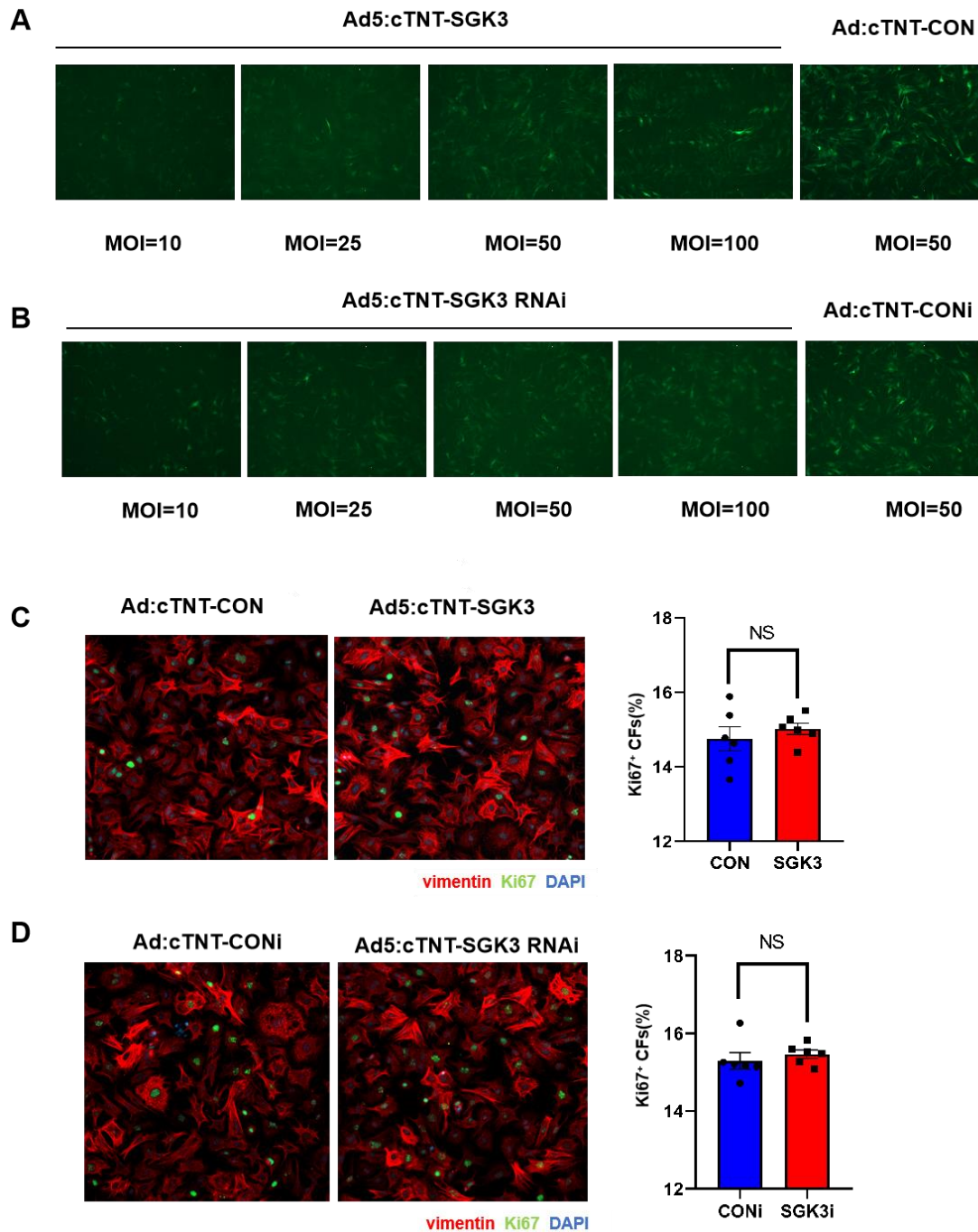
Figure S2. SGK3 homology analysis between human and mouse.

Query: Human- SGK3   Sbjct: mmu-SGK3

SGK3 homology analysis between human and mouse genome was conducted using

BLAST.

Figure S3. Selection of SGK3 CM-specific adenovirus transfection concentration and its effect on proliferation of cardiac fibroblasts.


A-B. Different titers (MOI = 10, 25, 50 and 100) of CM-specific SGK3 overexpression/knockdown associated adenovirus vector 5 (Ad5:cTNT-SGK3/ Ad5:cTNT-SGK3i) were used to transfect CMs for 48 hours. According to the fluorescence intensity, MOI = 50 was finally used as the appropriate transfection titer. C-D. Ki67^{+} immunofluorescence staining in primary neonatal cardiac fibroblasts (CFs) after SGK3 overexpression or SGK3 knockdown in CMs.

**Figure S4. The transfection efficiency of AAV9:cTNT-SGK3 in neonatal mice myocardial tissue.**
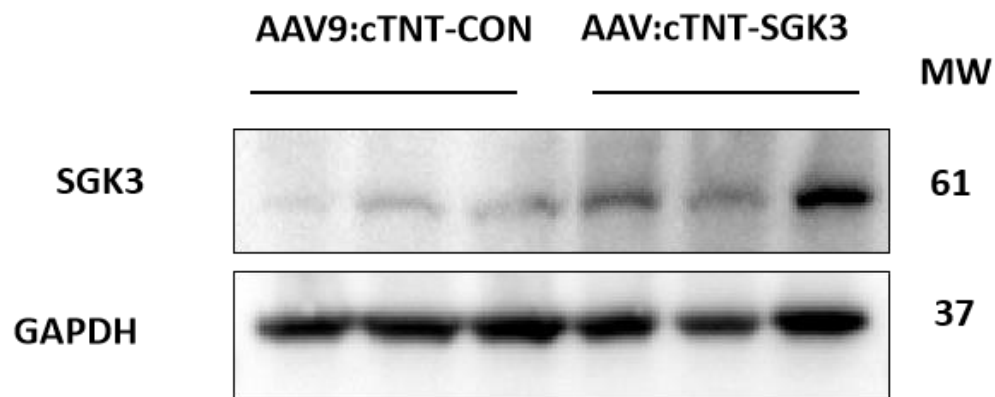
The AAV9:cTNT-SGK3 (1.1×10^{12} v.g/ml, total stock solution volume = 8 μl/mouse) or AAV9:cTNT-CON (1.1×10^{12} v.g/ml, total stock solution volume = 8 μl/mouse) intraperitoneally injected into P1 mice. After 14 days of intraperitoneal injection, western blot analysis was used to detect the expression of SGK3 between AAV9:cTNT-SGK3 and AAV9:cTNT-CON group myocardial tissue.

Figure S5. The transfection efficiency of Ad5:cTNT-SGK3 in neonatal mice post apical resection.

P1-AR: 6dpr
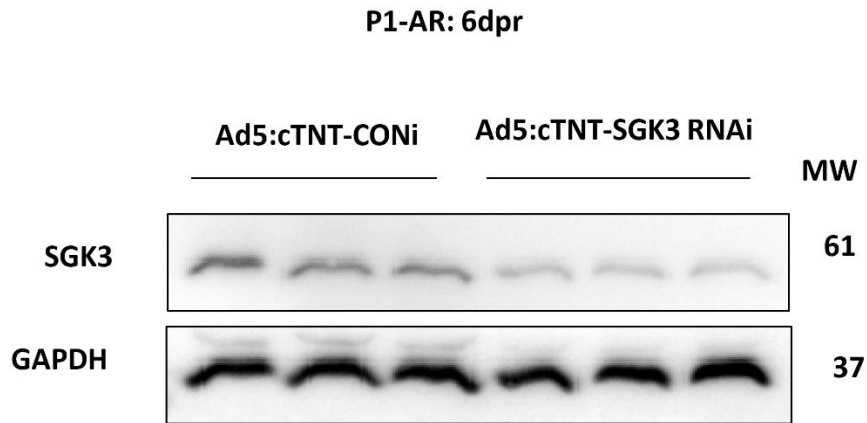
The Ad5:cTNT-SGK3i (2×10^{10} PFU/ml, total stock solution volume= 0.5 µl/mouse, diluted to 6 µl with PBS) or Ad5:cTNT-CONi (1×10^{11} PFU/ml, total stock solution volume= 0.1 µl/mouse, diluted to 6 µl with PBS) into three different locations around the apex (2 µl for each point) after apical resection (AR) in P1 mice using microinjector. At the 6-day after AR, western blot analysis was used to determine the expression of SGK3 between Ad5:cTNT-SGK3i and Ad5:cTNT-CONi group myocardial tissue.

Figure S6. The transfection efficiency of CM-specific SGK3 associated adenovirus and adeno-associated virus in adult myocardial tissue post ischemia reperfusion injury.
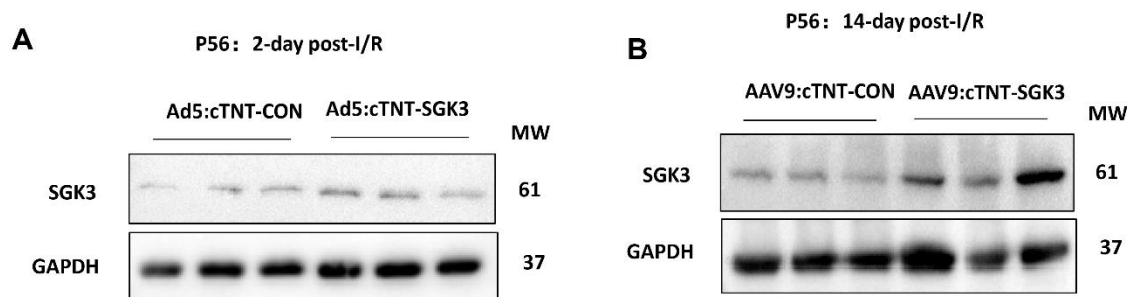
A. The Ad5:cTNT-SGK3 (2×10^{10} PFU/ml, total stock solution volume= 5 μl/mouse, diluted to 9 μl with PBS) or Ad5:CON (1×10^{11} PFU/ml, total stock solution volume= 1 μl/mouse, diluted to 9 μl with PBS) were injected into three different locations around the apex (3 μl for each point) post I/R injury in P56 mice. After 45 minutes of LAD ligation, the suture was untied to allow reperfusion. Western blot analysis was used to determine the expression of SGK3 between Ad5:cTNT-SGK3 and Ad5:cTNT-CON group myocardial tissue at 2-day post I/R. B. The AAV9:cTNT-SGK3 (1.1×10^{12} v.g/ml, total stock solution= 1 μl/mouse, diluted to 9 μl with PBS) or AAV9:CON (1.1×10^{12} v.g/ml, total stock solution= 1 μl/mouse, diluted to 9 μl with PBS) into three locations (3 μl for each point) of infarct border myocardium after ischemia. Western blot analysis was used to determine the expression of SGK3 between AAV9:cTNT-SGK3 and AAV9:cTNT-CON group myocardial tissue at 14-day post I/R.

Figure S7. SGK3 regulates CM proliferation via GSK-3β/β-catenin pathway *in vitro.*
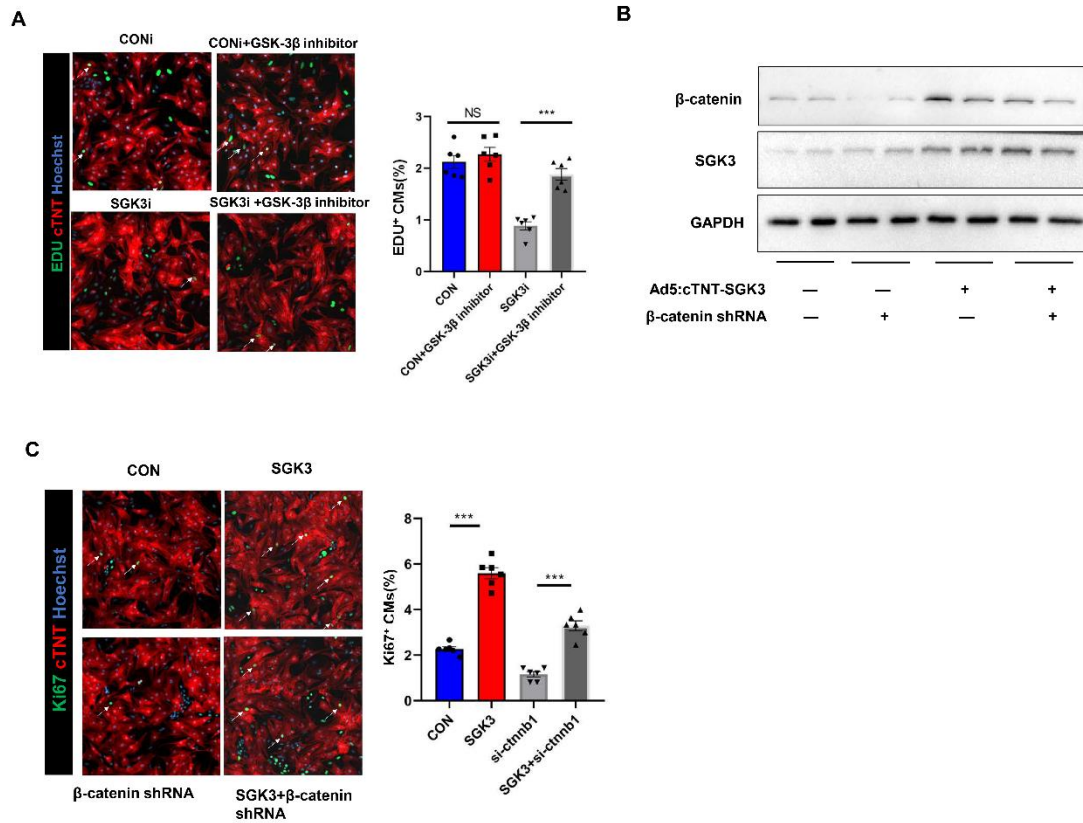
A. BIO (2μM), an inhibitor of GSK-3β, treated CMs with or without Ad5:cTNT-SGK3 for 48 hours. Immunofluorescence staining was then used to confirm the CM proliferation for EDU[+] (5902 CMs in Ad5:CON group, 4907 CMs in BIO group, 5674 CMs in Ad5:SGK3i group and 5647 CMs in Ad5:SGK3i+BIO group, n=6). B. The CMs were transfected with SGK3 alone or with β-catenin shRNA for 48 hours, the transfection efficiency was proved by western blot analysis. C. Immunofluorescence staining of CMs *in vitro* was used to confirm the CM proliferation for Ki67^{+} (3604 CMs in Ad5:CON group, 3701 CMs in β-catenin shRNA group, 3416 CMs in Ad5:cTNT-SGK3 group and 3367 CMs in Ad5:cTNT-SGK3+β-catenin shRNA group, n=6). Data are presented as mean± SEM. ***P≤0.001; NS: no significance.